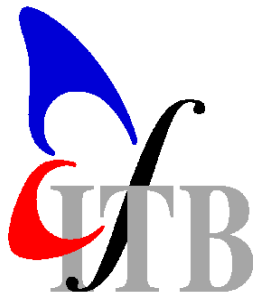


The circadian clock – a system of coupled oscillators



Hanspeter Herzel

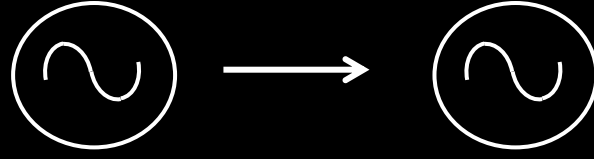
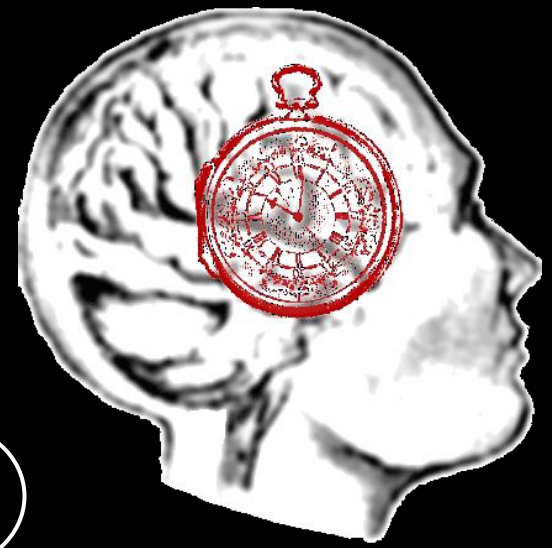
Institute for Theoretical Biology (ITB)
Charité and Humboldt University Berlin

together with

Patrick Pett, Grigory Bordyugov, Bharath Ananthasubramaniam,
Christoph Schmal (ITB), Achim Kramer group (Charite), Anja
Korencic (Ljubljana), Isao Tokuda (Kyoto), Adrian Granada (Harvard)



Zeitgeber
Light
Temperature
Food
...



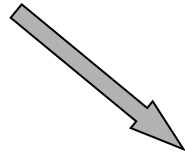
The environmental **external oscillator**

entrains

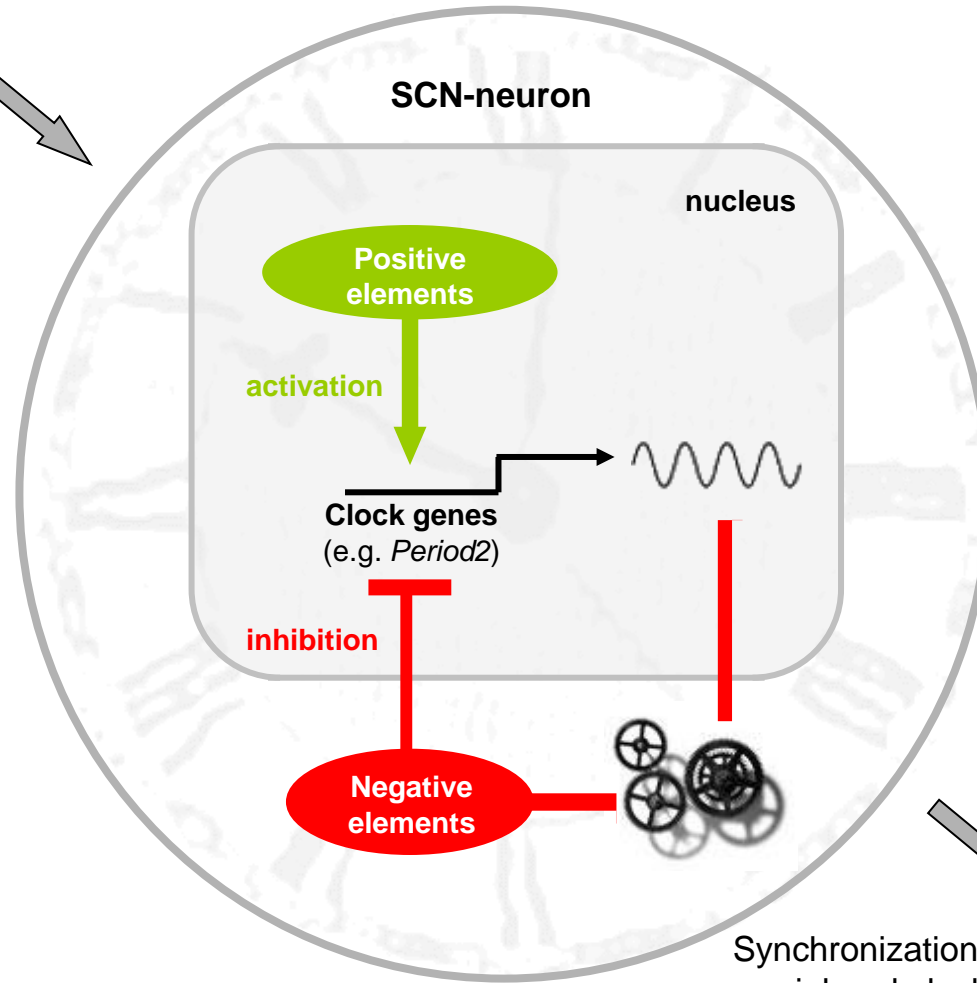
our **internal oscillator**
(the circadian clock)



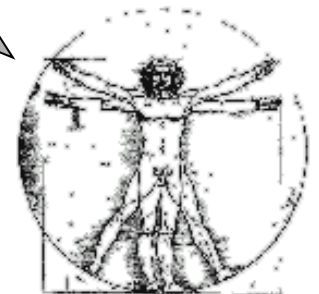
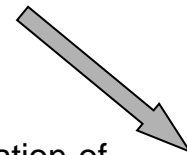
Light synchronizes the clock



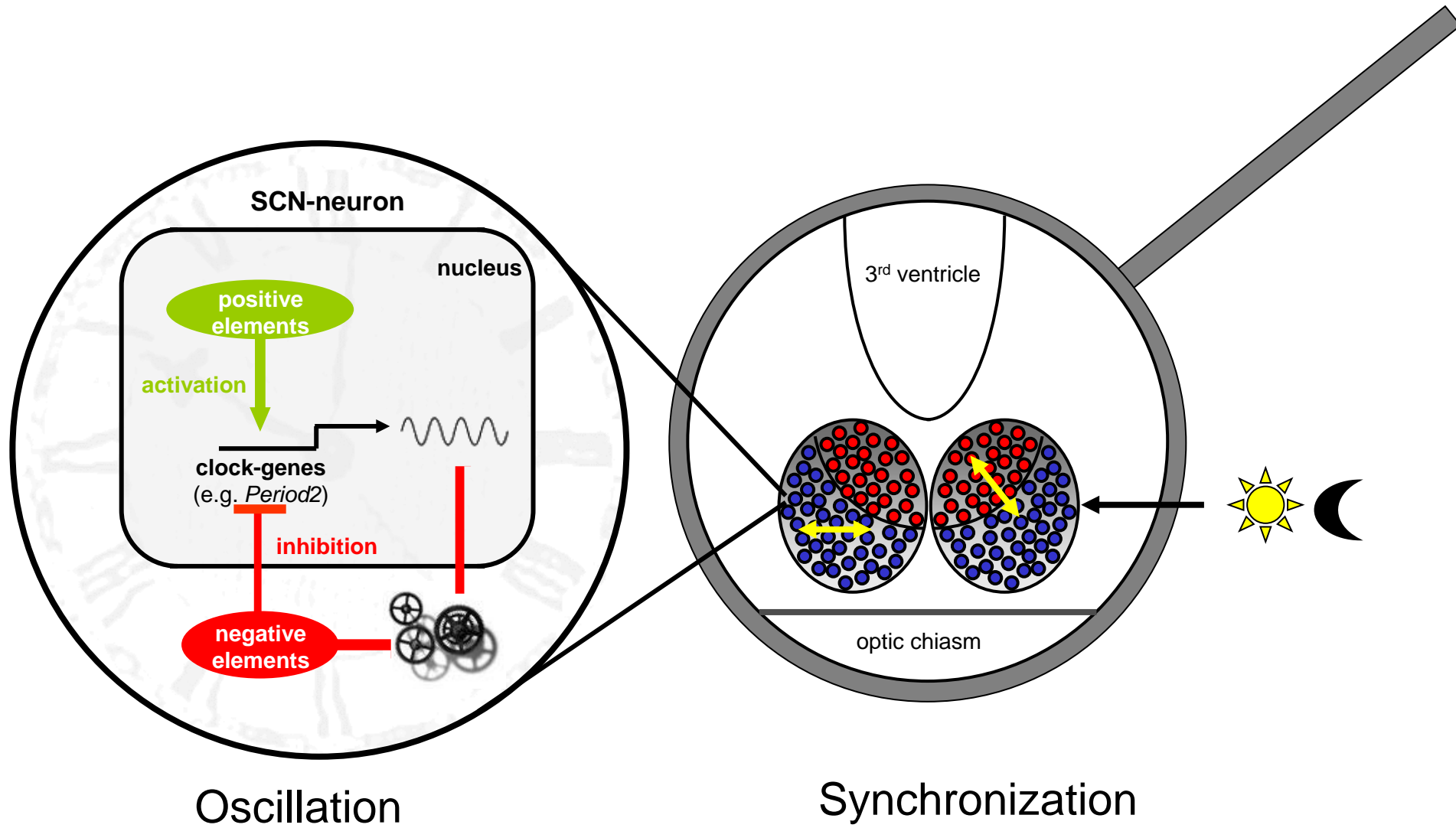
The system



Regulation of physiology and behavior

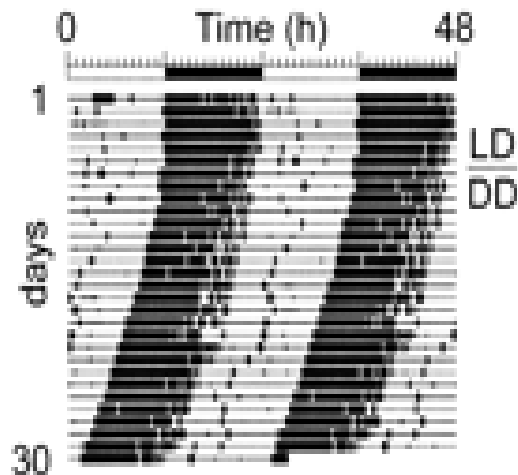


Molecular Chronobiology

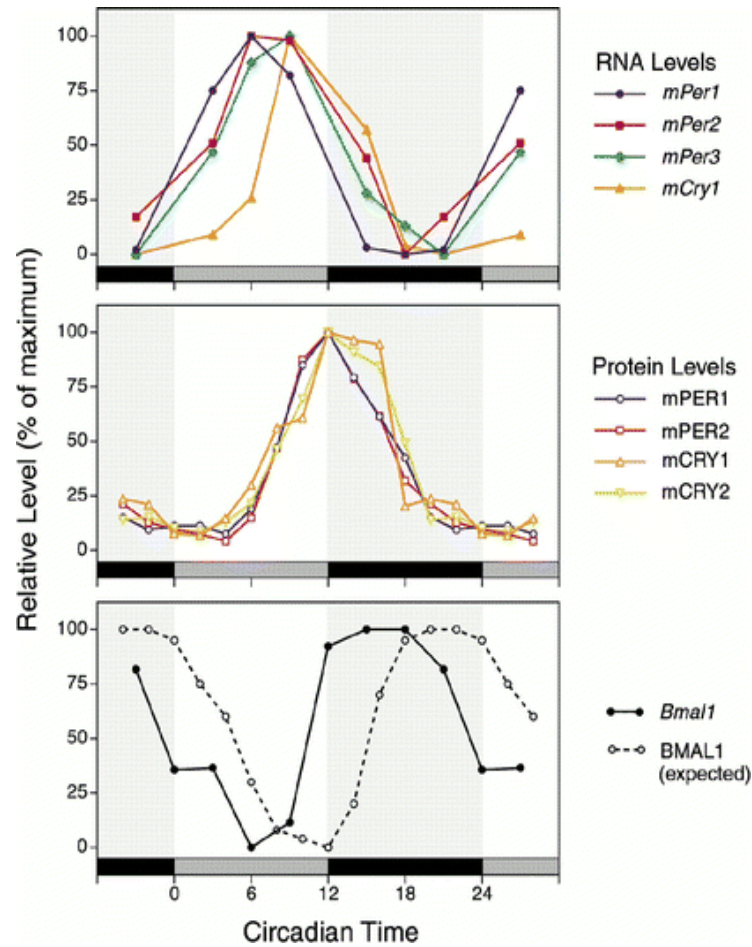


The circadian oscillator

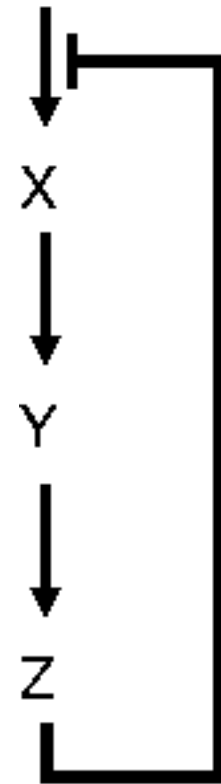
Circadian rhythm ← Oscillations ← Feedback loops



Oster et al., 2002

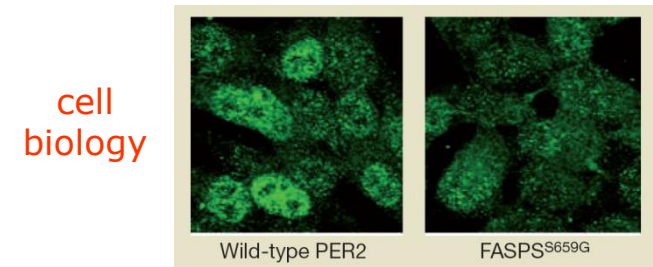
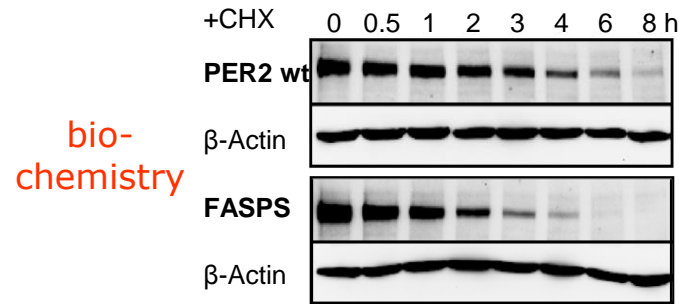
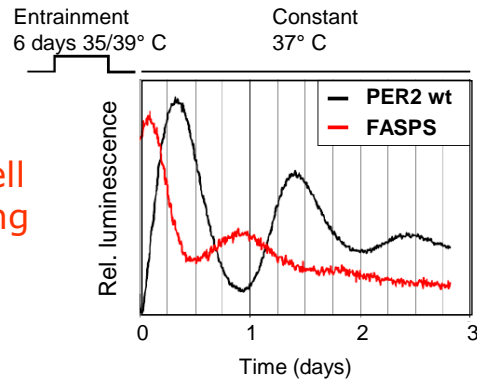
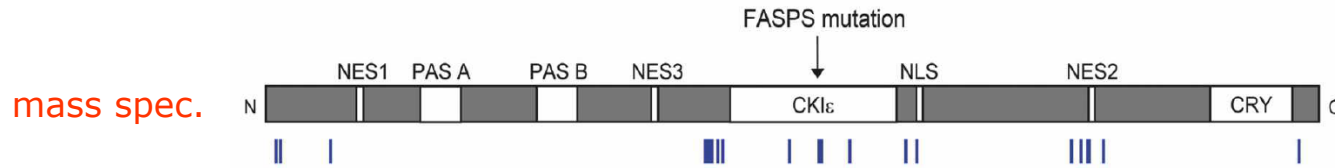


Reppert and Weaver, 2001

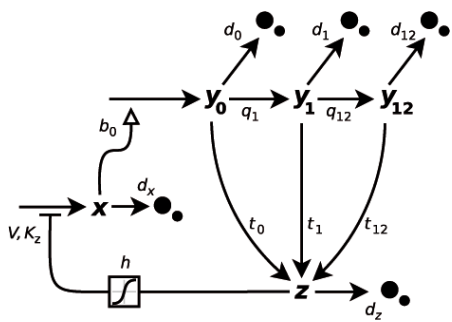


Molecular Chronobiology

Measurements



Mathematical Model



$$\dot{x} = \frac{V}{1 + \left(\frac{z}{K_z}\right)^h} - d_x x$$

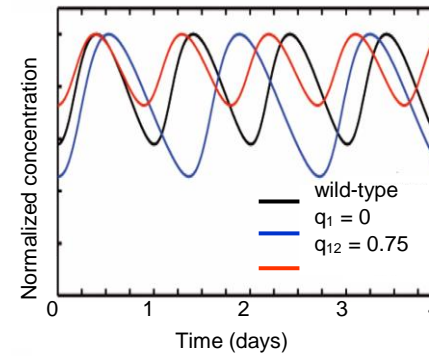
$$\dot{y}_0 = b_0 x - (d_0 + t_0 + q_1) y_0$$

$$\dot{y}_1 = q_1 y_0 - (d_1 + t_1 + q_{12}) y_1$$

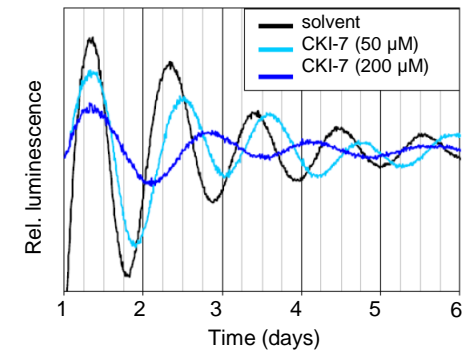
$$\dot{y}_{12} = q_{12} y_1 - (d_{12} + t_{12}) y_{12}$$

$$\dot{z} = t_0 y_0 + t_1 y_1 + t_{12} y_{12} - d_z z$$

Model prediction

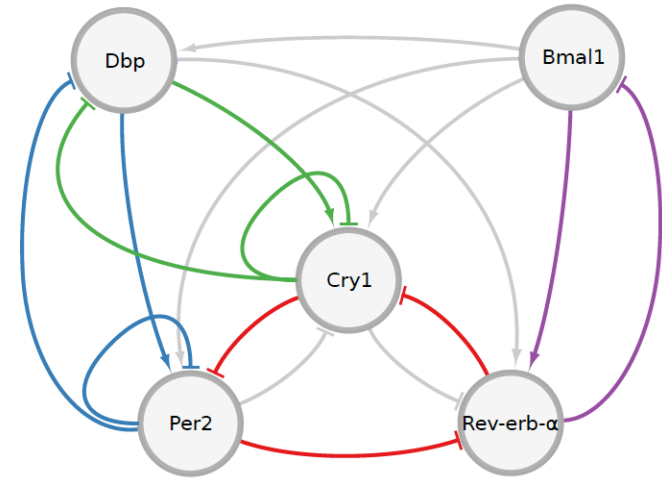


Test of prediction

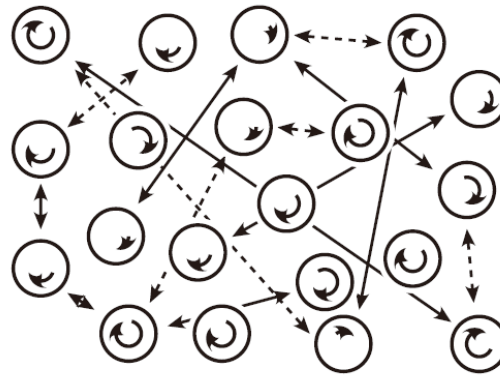


Coupled oscillators

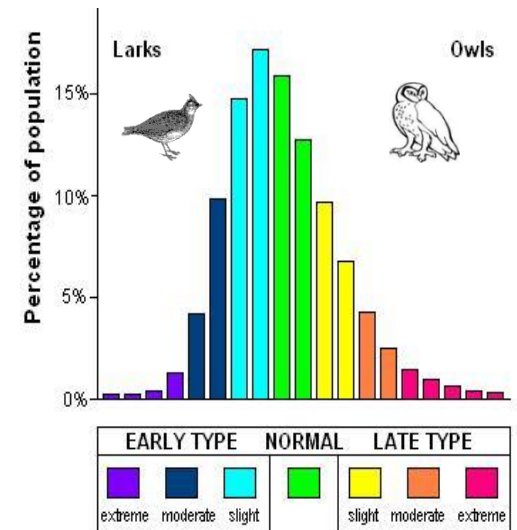
1. Synergy of feedback loops



2. Oscillator networks



3. Entrainment phase (chronotypes)



Clock genes and feedback loops

Proc. Nat. Acad. Sci. USA
Vol. 68, No. 9, pp. 2112-2116, September 1971

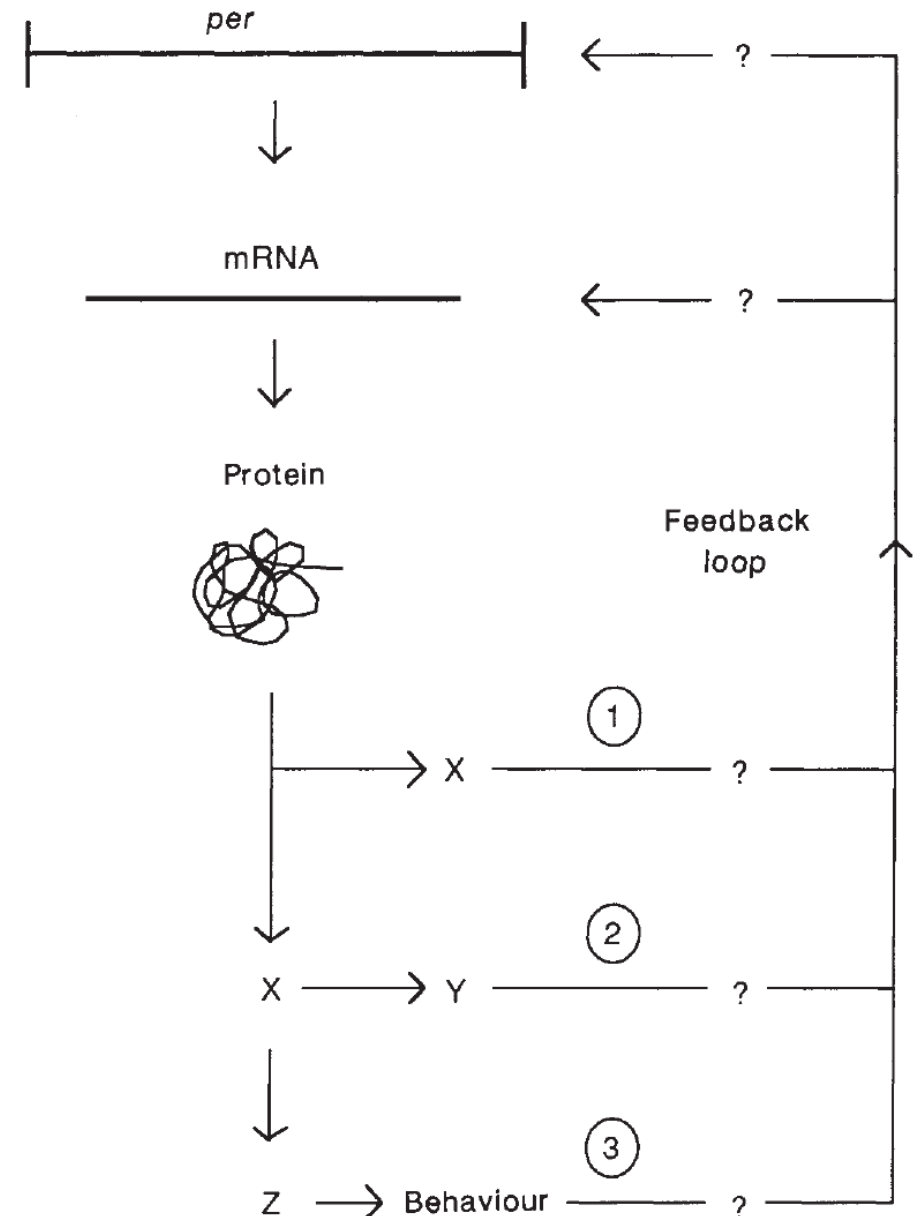
Clock Mutants of *Drosophila melanogaster*

(eclosion/circadian/rhythms/X chromosome)

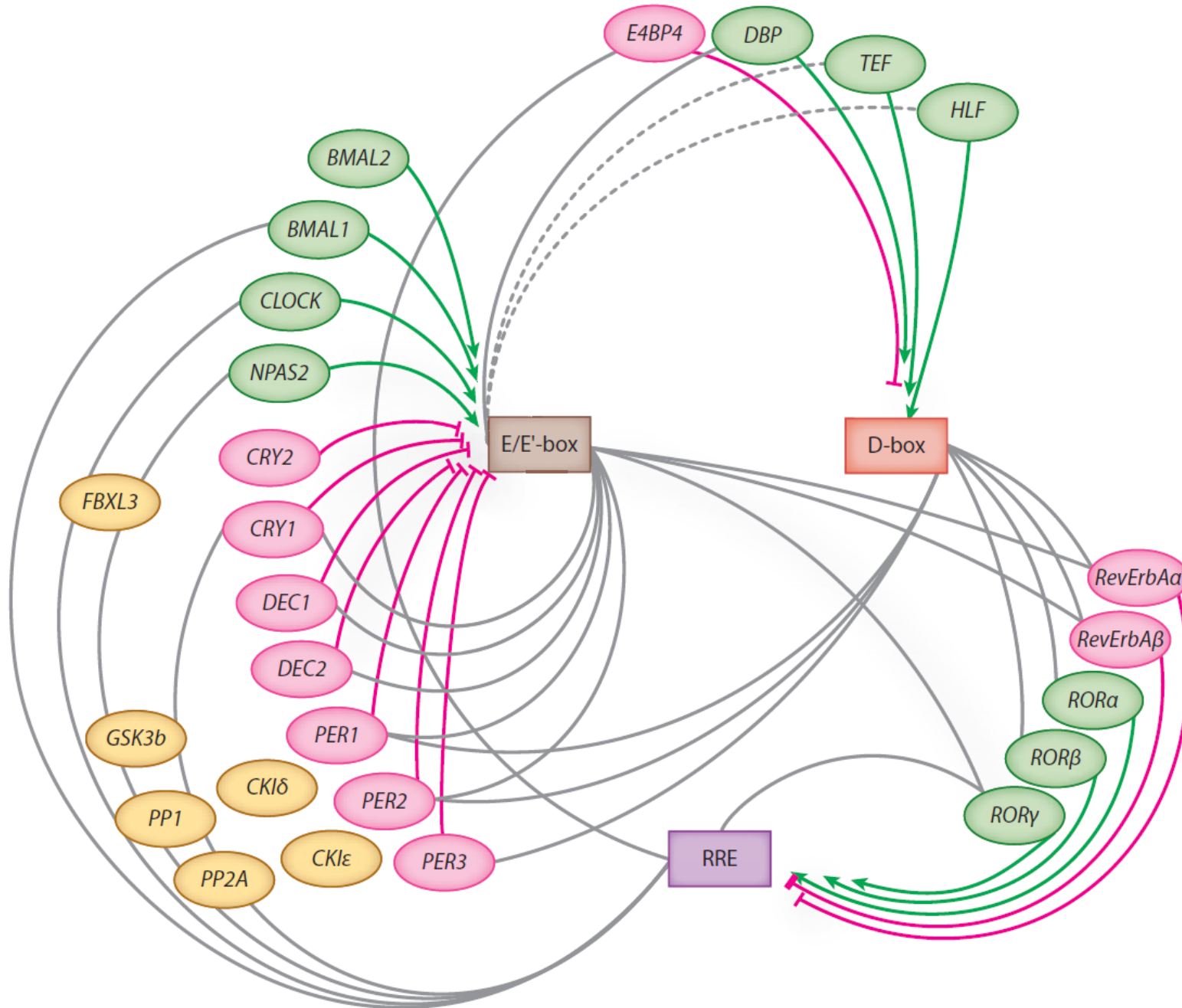
RONALD J. KONOPKA AND SEYMOUR BENZER

Feedback of the *Drosophila period* gene product on circadian cycling of its messenger RNA levels

Paul E. Hardin^{*†}, Jeffrey C. Hall[†] & Michael Rosbash^{*†}

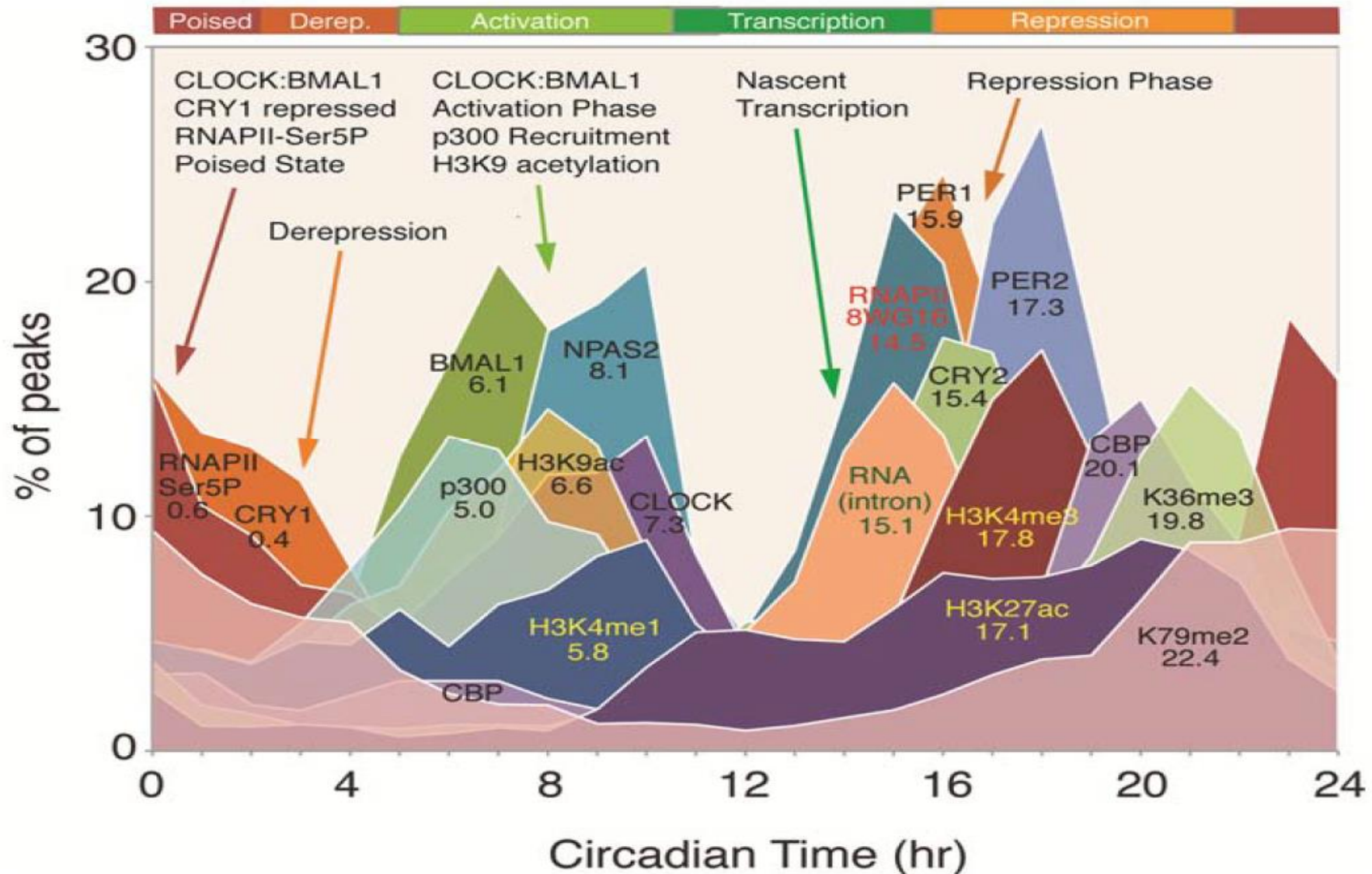


E-boxes, ROR-elements and D-boxes drive clock genes



Transcriptional Architecture and Chromatin Landscape of the Core Circadian Clock in Mammals

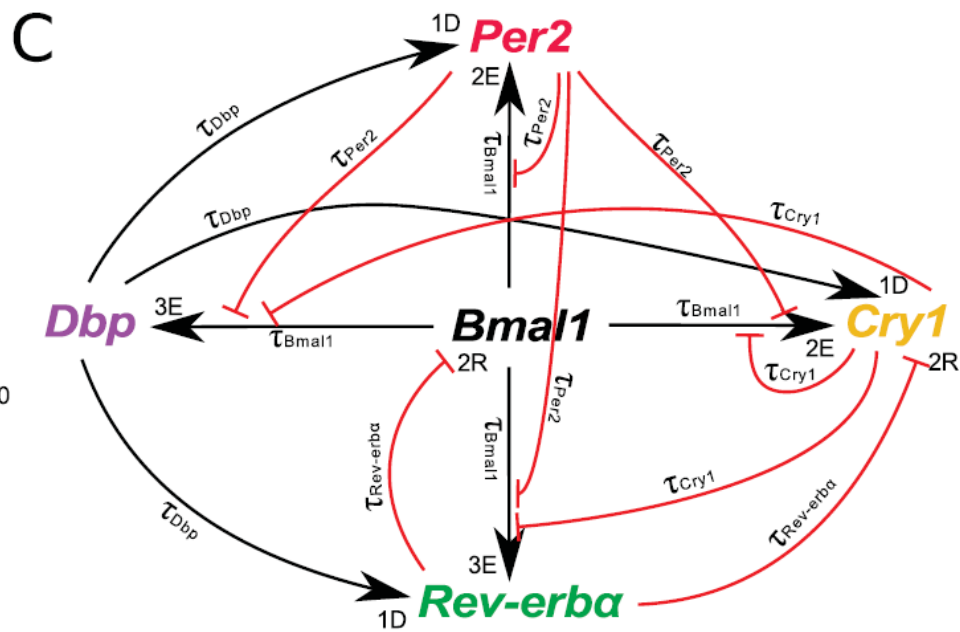
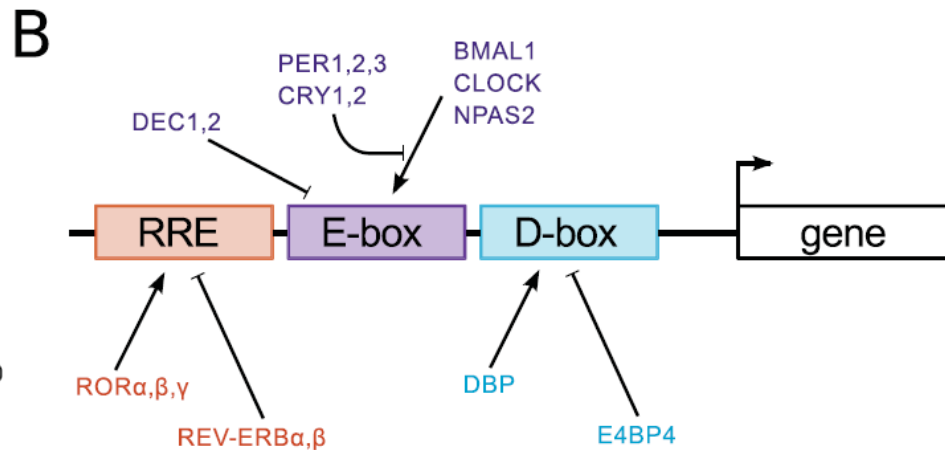
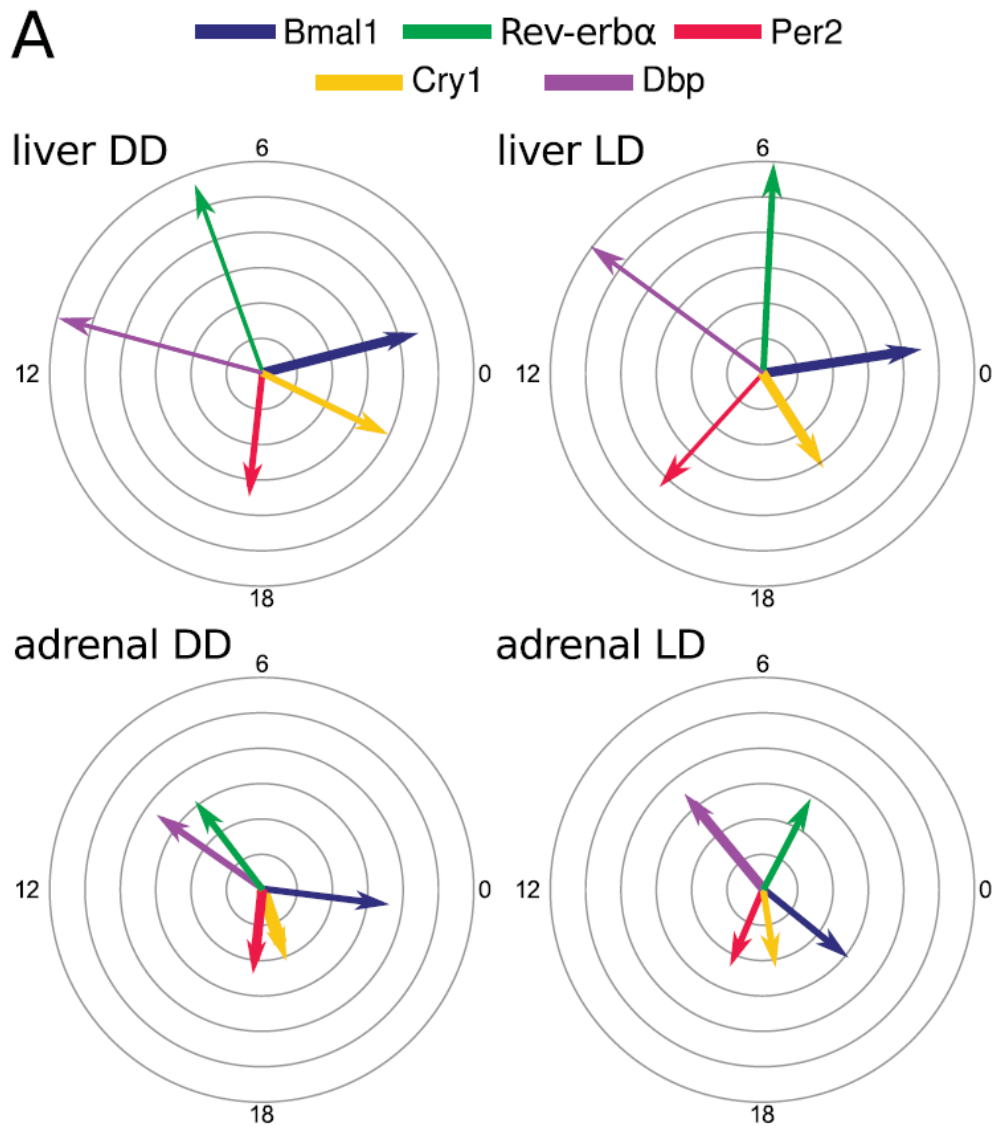
Nobuya Koike,¹ Seung-Hee Yoo,¹ Hung-Chung Huang,¹ Vivek Kumar,¹ Choogon Lee,² Tae-Kyung Kim,¹ Joseph S. Takahashi^{1,3*}



Construction of a core clock model using

- representative genes: activators (Bmal1, Dbp)+ early inhibitors (Per2, Rev-Erb)+late inhibitor (Cry1)
- experimentally verified binding sites
- known degradation rates
- reasonable delays
- fitted transcriptional parameters

Core-clock model from expression profiles and promoters



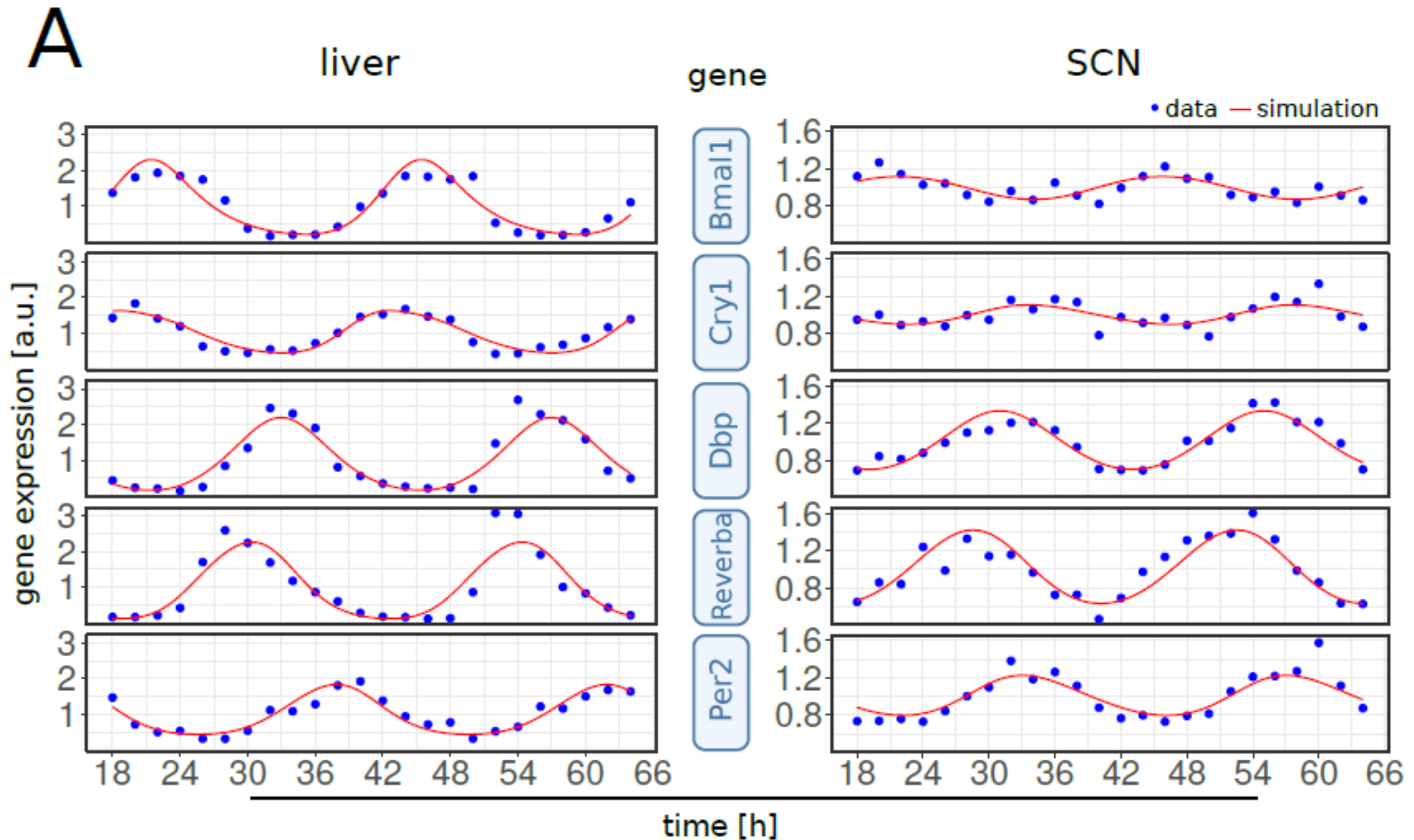
Model design and global optimization

$$\frac{d [RevErb_{\alpha}]}{dt} = \underbrace{\left(\frac{\frac{b_RevErb [Bmal1](t-del1)}{ba2} + 1}{\frac{[Bmal1](t-del1)}{ba2} + 1} \right)^3}_{Bmal1 (+)} \underbrace{\left(\frac{1}{\frac{[Per2](t-del3)}{cr2} + 1} \right)^3}_{Per2 (-)} \underbrace{\left(\frac{\frac{f_RevErb [Dbp](t-del5)}{fa2} + 1}{\frac{[Dbp](t-del5)}{fa2} + 1} \right)^3}_{Dbp (+)} \underbrace{\left(\frac{1}{\frac{[Cry1](t-del4)}{gr2} + 1} \right)^3}_{Cry1 (-)} -d2 [RevErb_{\alpha}] (t)$$

$$score = \frac{(period_{sim} - period_{exp})^2}{tol_{period}^2} + \sum \frac{(phase_{sim} - phase_{exp})^2}{tol_{phase}^2} + \sum \frac{(foldch_{sim} - foldch_{exp})^2}{tol_{foldch}^2}$$

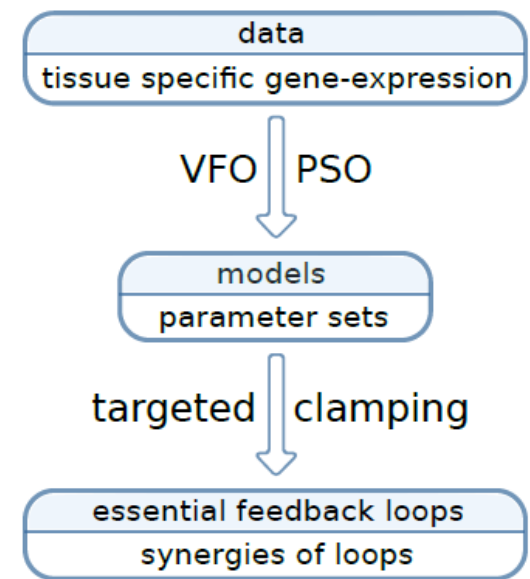
- Delays (h): [0, 6]
- Degradation rates: [0, 1]

5 DDE model can reproduce expression profiles



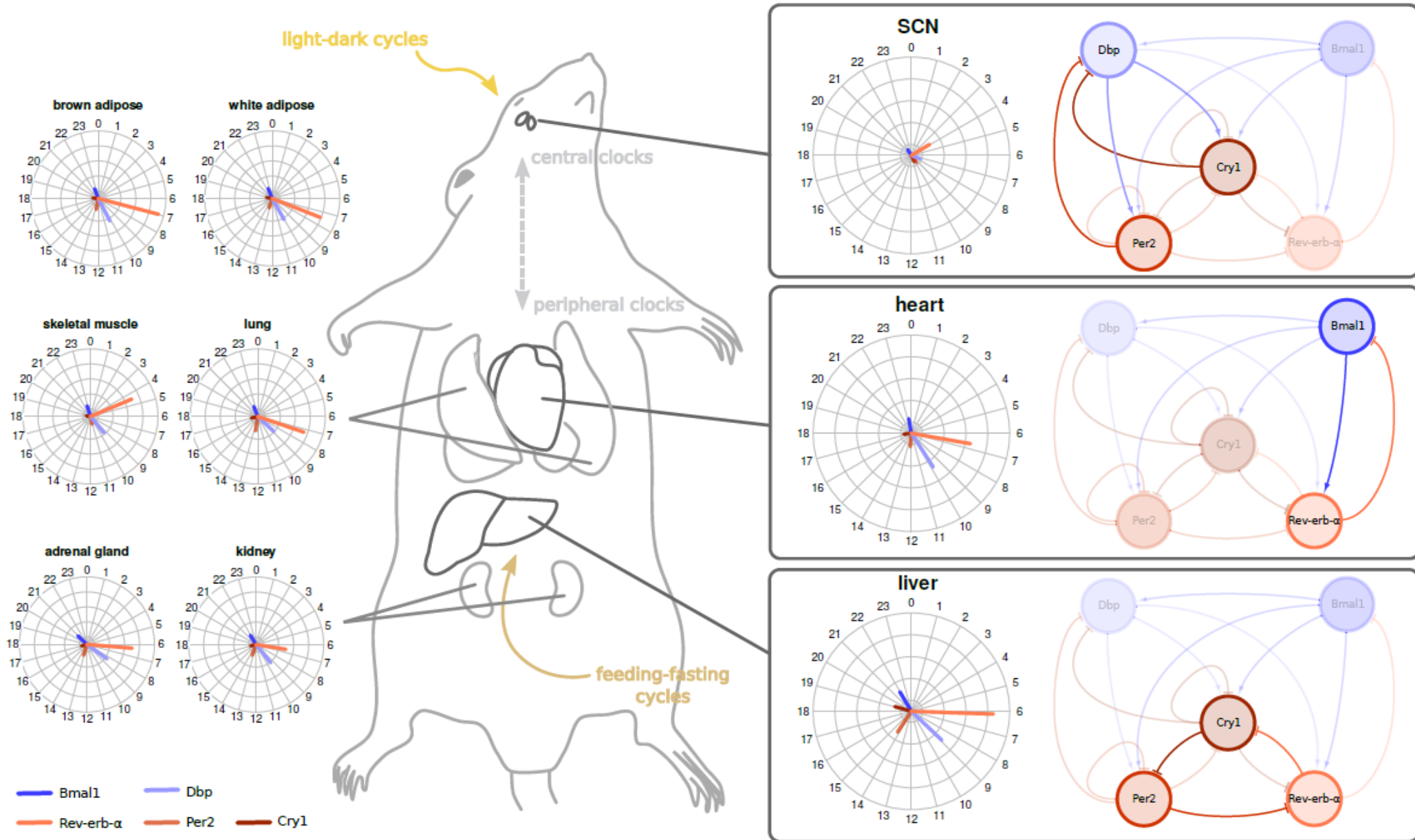
Global optimization finds multiple parameter sets

P. Pett et al.: Co-existing feedback loops generate tissue-specific circadian rhythms, submitted



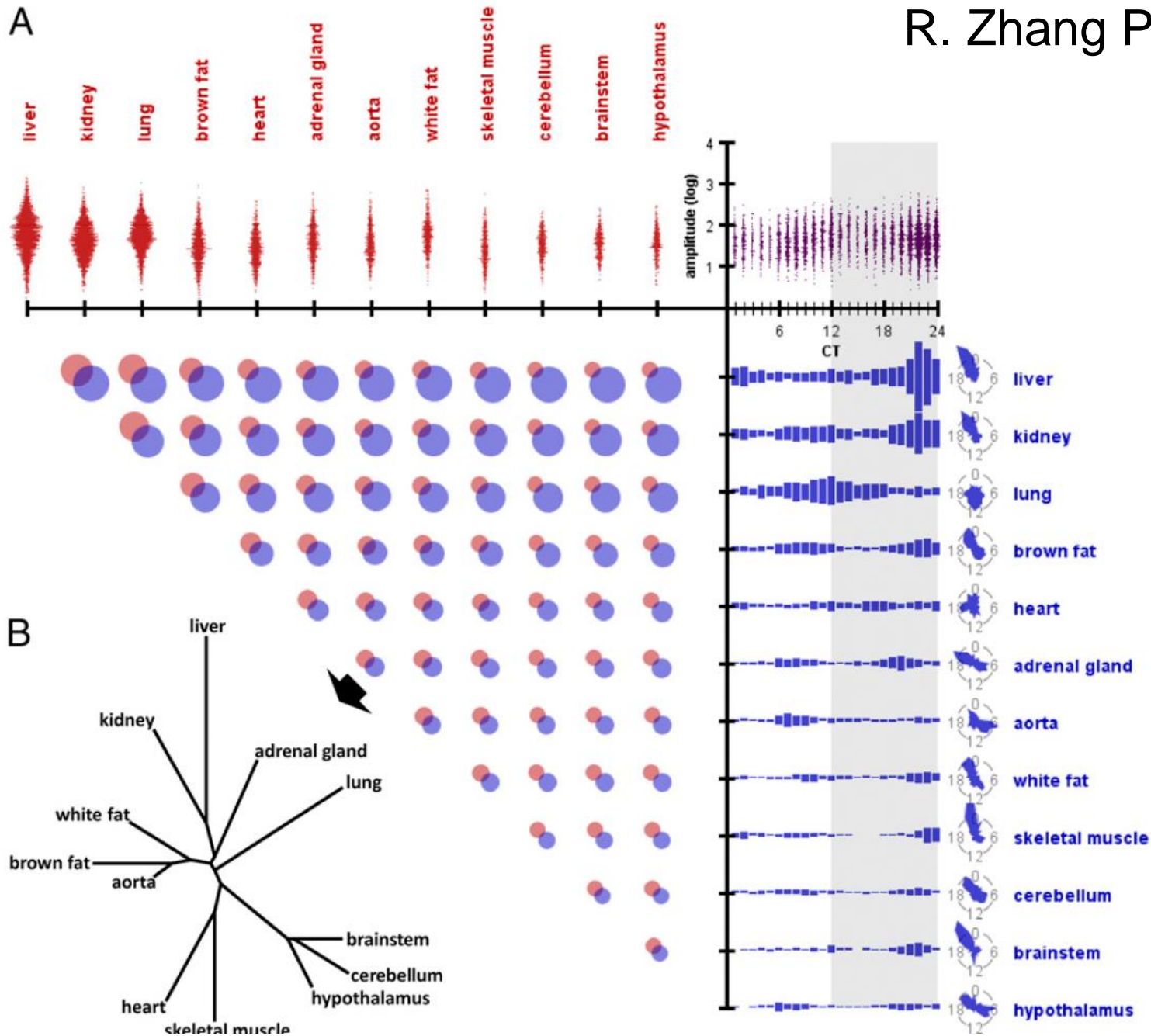
	adrenal gland	kidney	liver	heart	skeletal muscle	lung	brown adipose	white adipose	SCN	cerebellum
number of runs	100	93	57	57	58	31	62	45	153	58
runs with score < 10	66	59	52	44	35	21	36	22	46	39
mean score	3.84	4.48	1.58	3.74	5.17	3.04	4.00	3.24	7.21	3.99

Synergy of feedback loops allows tissue specificity

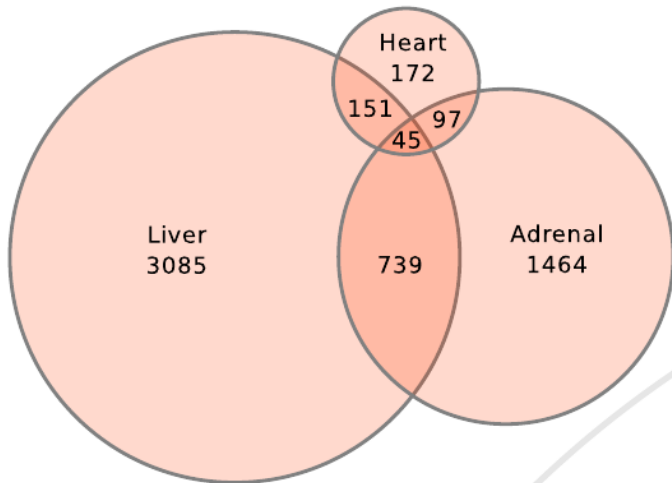


Large tissue diversity of peripheral clocks

R. Zhang PNAS 2014



Clock-controlled genes in peripheral organs

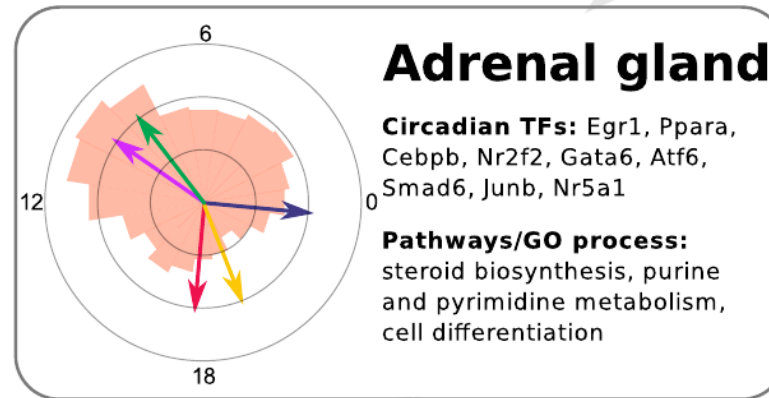


Common rhythmic TFs:
Arntl, Bhlhe40, Dbp, Hes6, Nfil3, Nr1d1, Nr1d2, Tef

direct: ANS
indirect: body T, metabolism, neuroendocrine signals

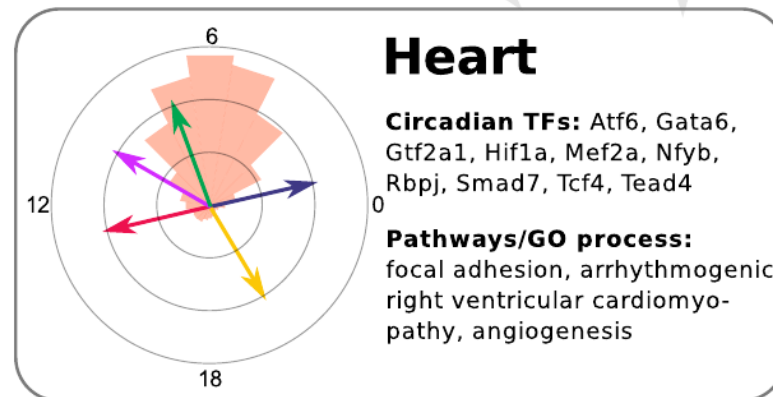
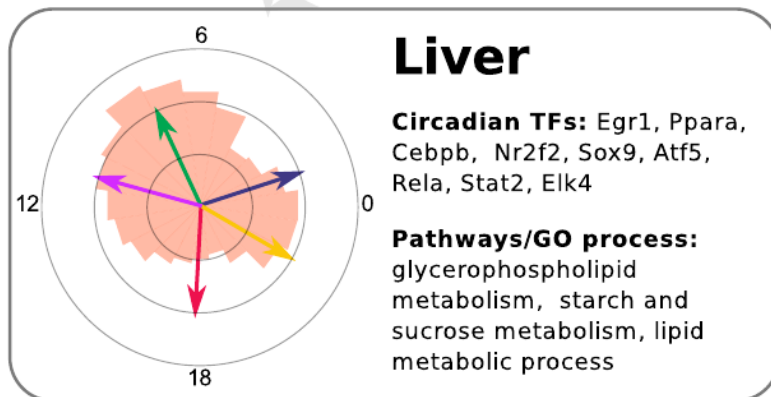
SCN

indirect: hormonal signals (HPA axis)
direct: ANS



direct: ANS
indirect: body T, activity, neuroendocrine signals

glucocorticoids



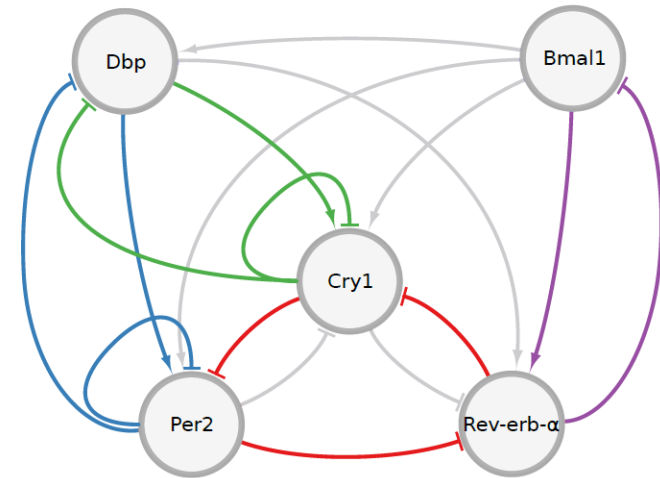
Summary Part 1

How to design a minimal core clock model?

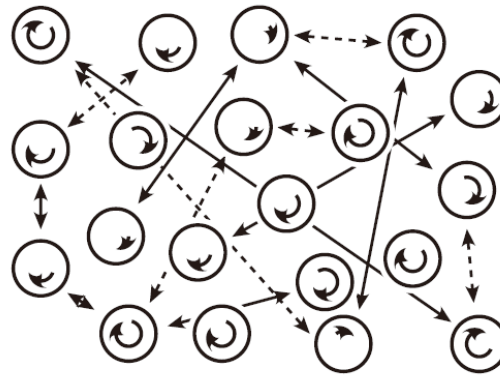
- Five genes represent most regulations
- DDEs require few parameters
- Transcriptional regulations remain heuristic
- Per/Cry loops, Rev-Erba loop and repressilator possible
- Peripheral tissues: comparable core clock but different clock-controlled genes and tissue-specific timing

Outline

1. Synergy of feedback loops



2. Oscillator networks



3. Entrainment phase (chronotypes)

Paradigm 2004: single cells are self-sustained, periods vary from 20 to 28 hours, weak coupling

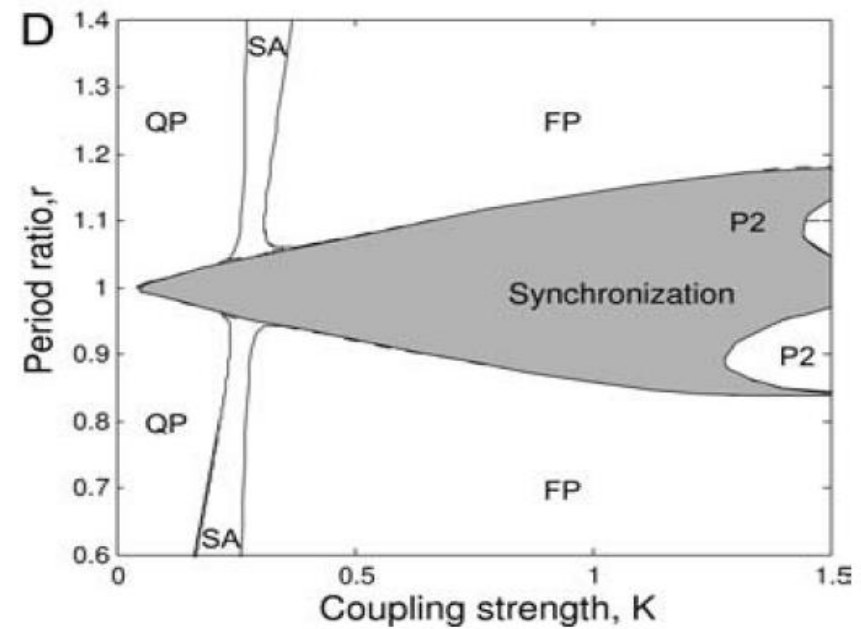
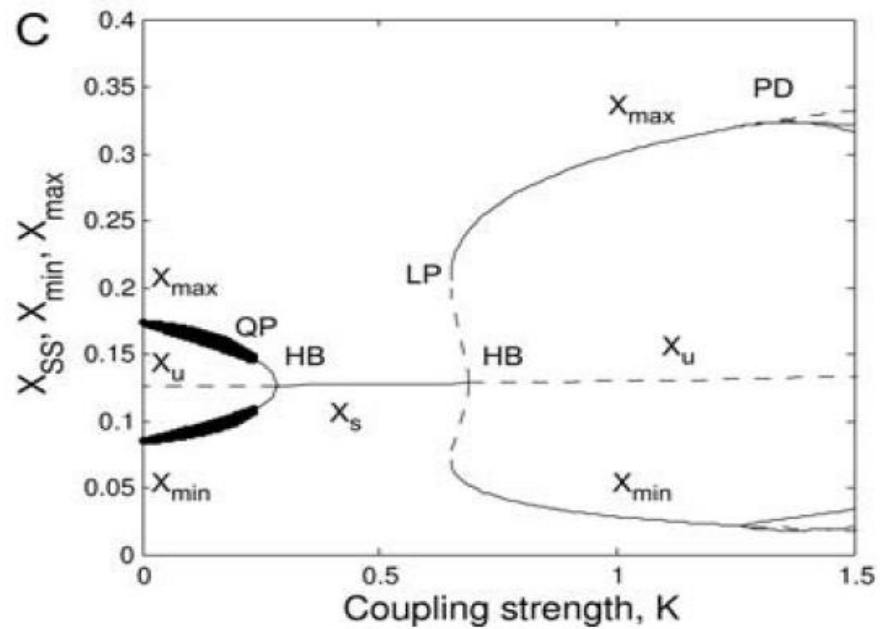
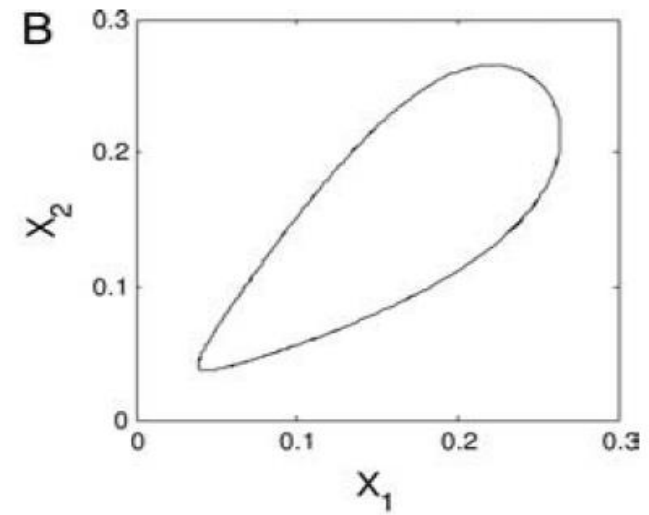
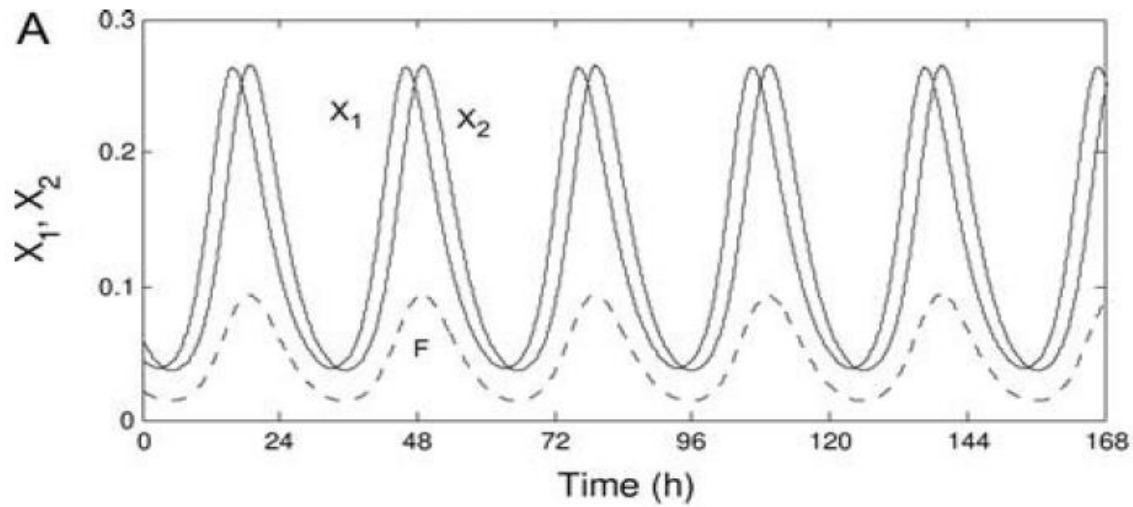
Nonlinear dynamics: tori, chaos ... expected

Observations: - 20000 neurons in the SCN are robustly synchronized

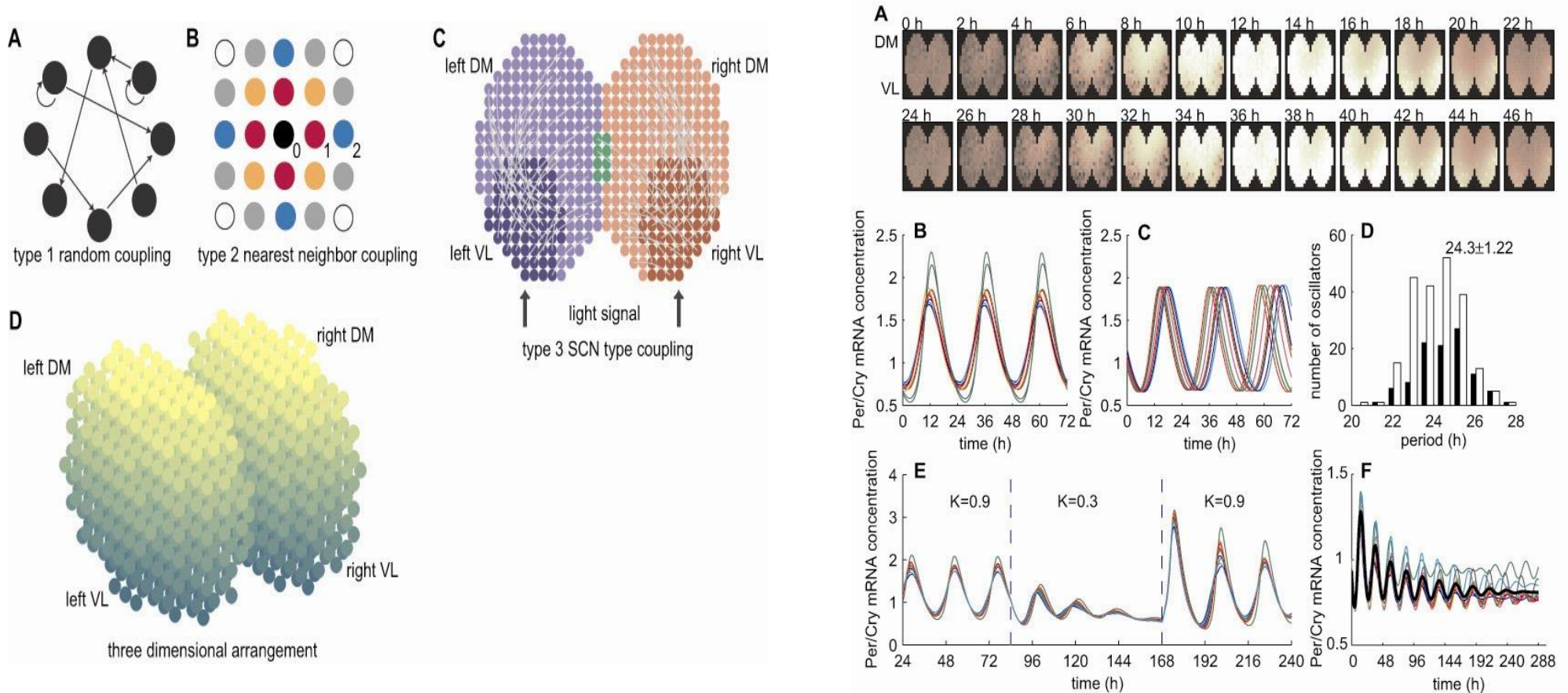
- „splitting“ rare

Bifurcation diagram of coupled Goodwin models

Synchronization of Circadian Oscillators

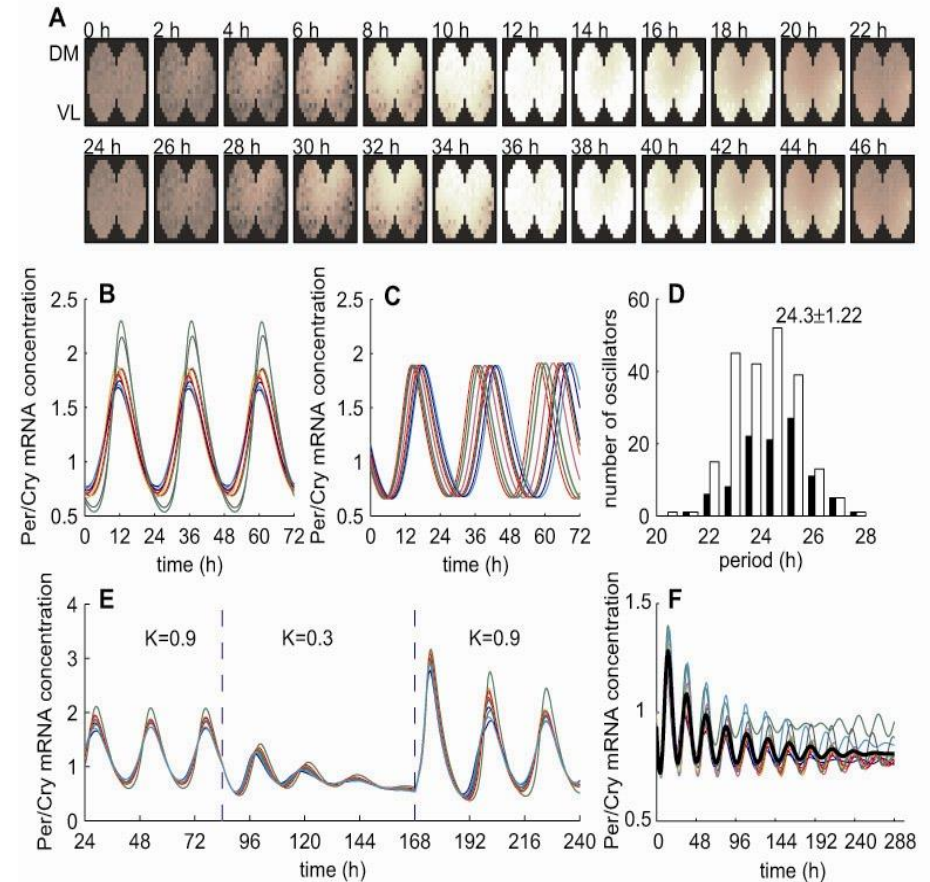
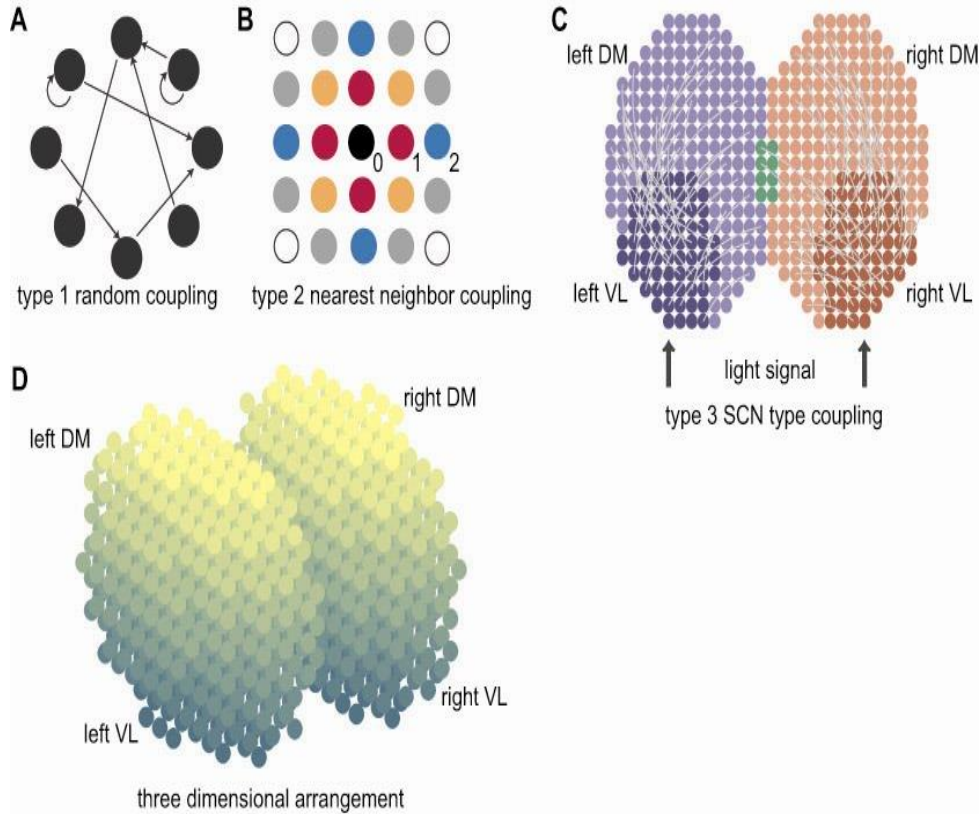


Sloppy oscillators synchronize well independent of specific coupling scheme



S. Bernard, D. Gonze, B. Cajavec, H. Herzl, and A. Kramer: Synchronization-Induced Rhythmicity of Circadian Oscillators in the Suprachiasmatic Nucleus, PLoS Comp. Biol. (2007) 3:e68.

Damped oscillators synchronize well independent of specific coupling scheme



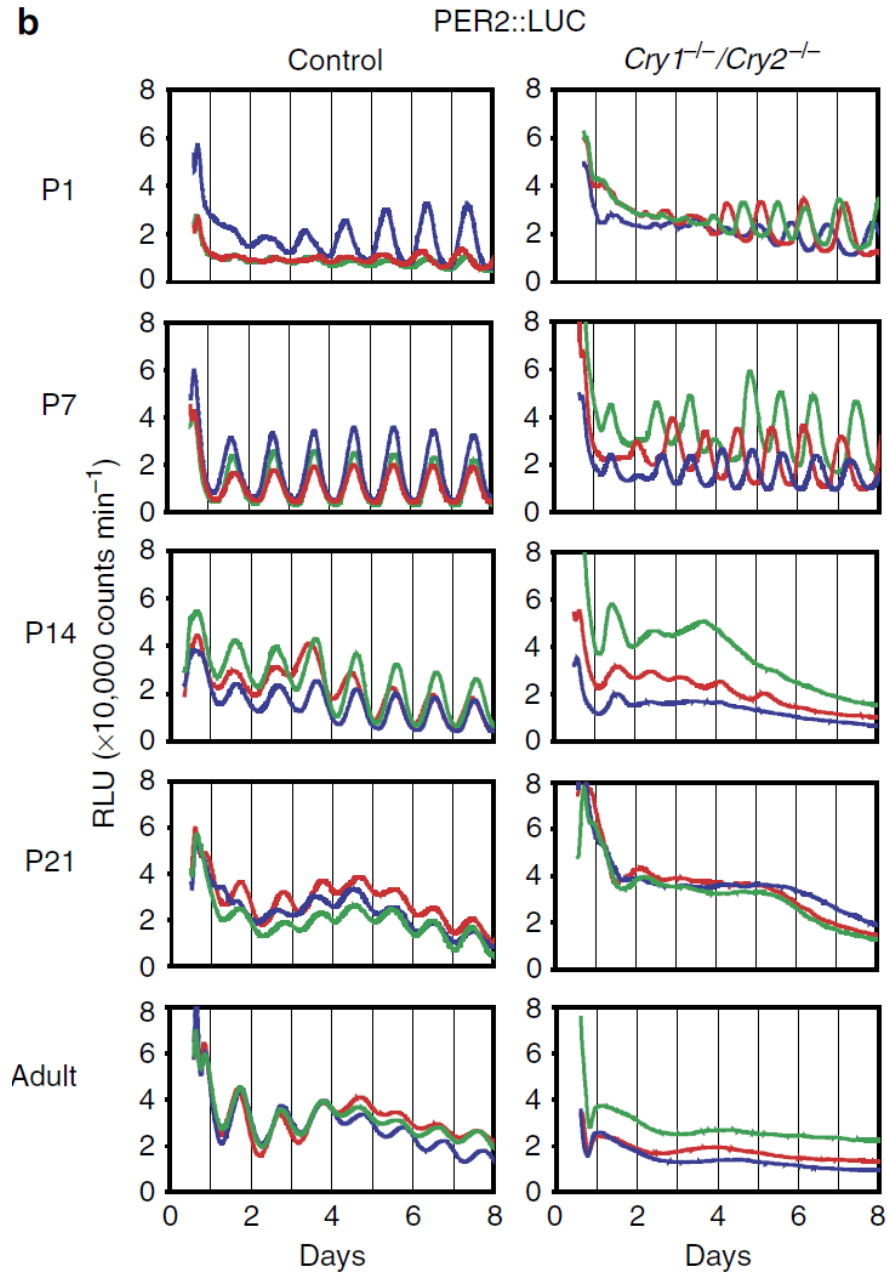
S. Bernard, D. Gonze, B. Cajavec, H. Herzog, and A. Kramer: Synchronization-Induced Rhythmicity of Circadian Oscillators in the Suprachiasmatic Nucleus, *PLoS Comp. Biol.* (2007) 3:e68.

Intrinsic, nondeterministic circadian rhythm generation in identified mammalian neurons

Alexis B. Webb^a, Nikhil Angelo^a, James E. Huettnner^b, and Erik D. Herzog^{a,1}

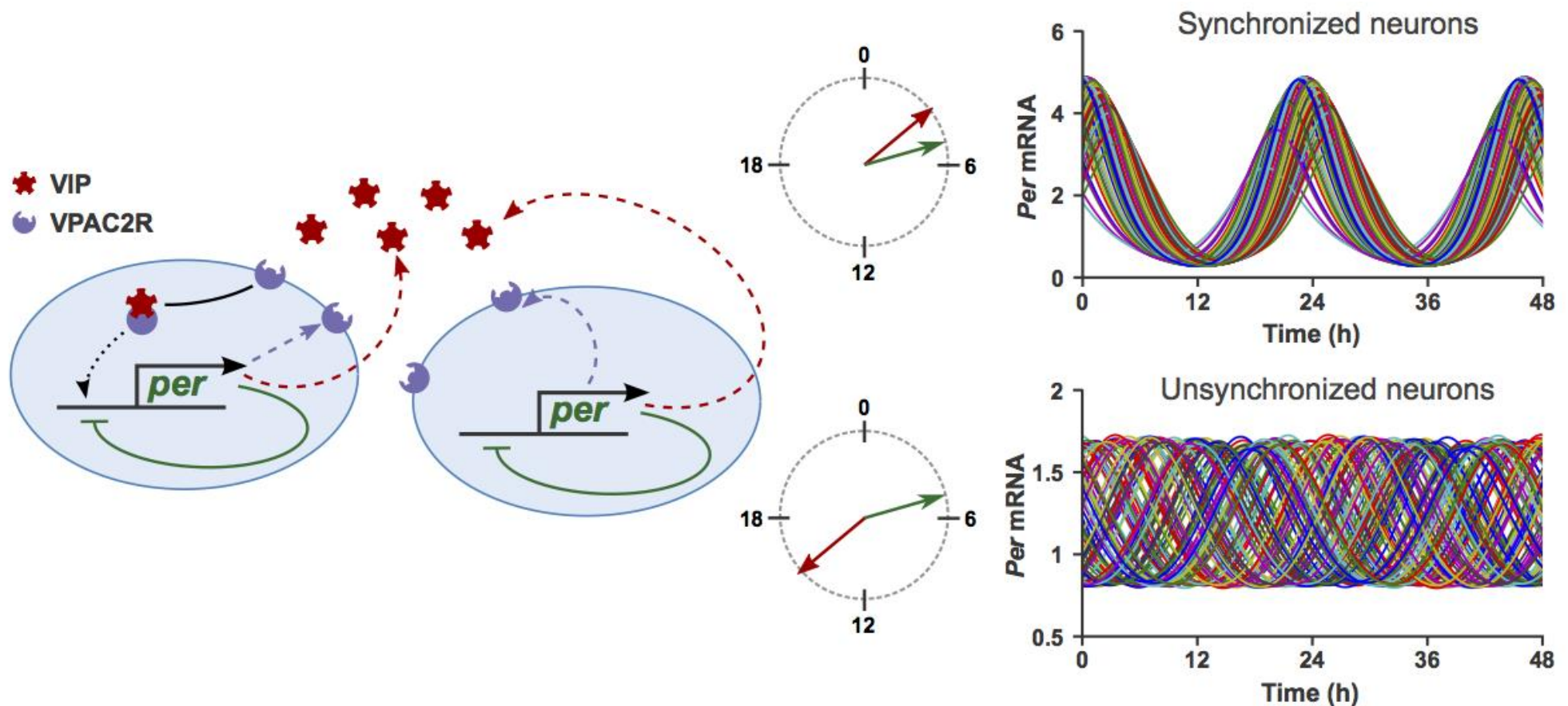
makers. Instead, these results indicate that AVP, VIP, and other SCN neurons are intrinsic but unstable circadian oscillators that rely on network interactions to stabilize their otherwise noisy cycling.

Coupling can even synchronize Cry-DKO neonatal SCN



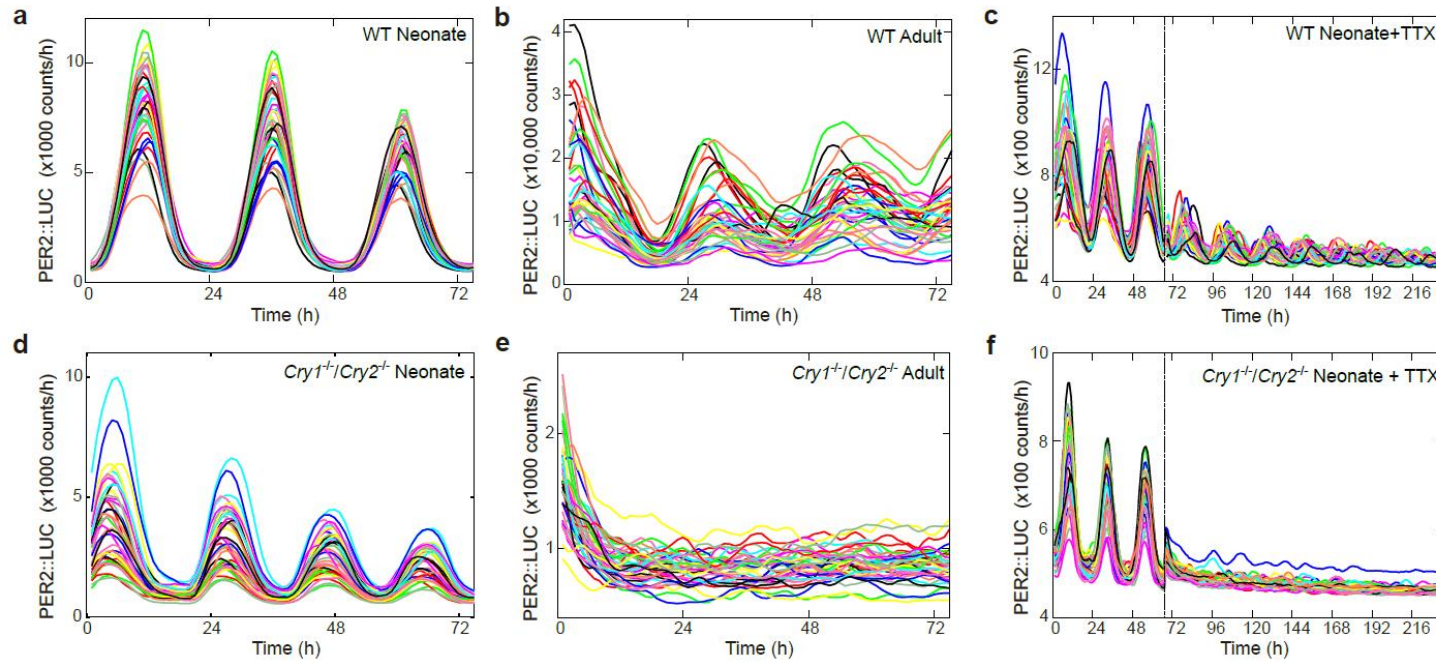
D. Ono, S. Honma, K. Honma
Nature Communications 2013

Coupling phase controls synchronization

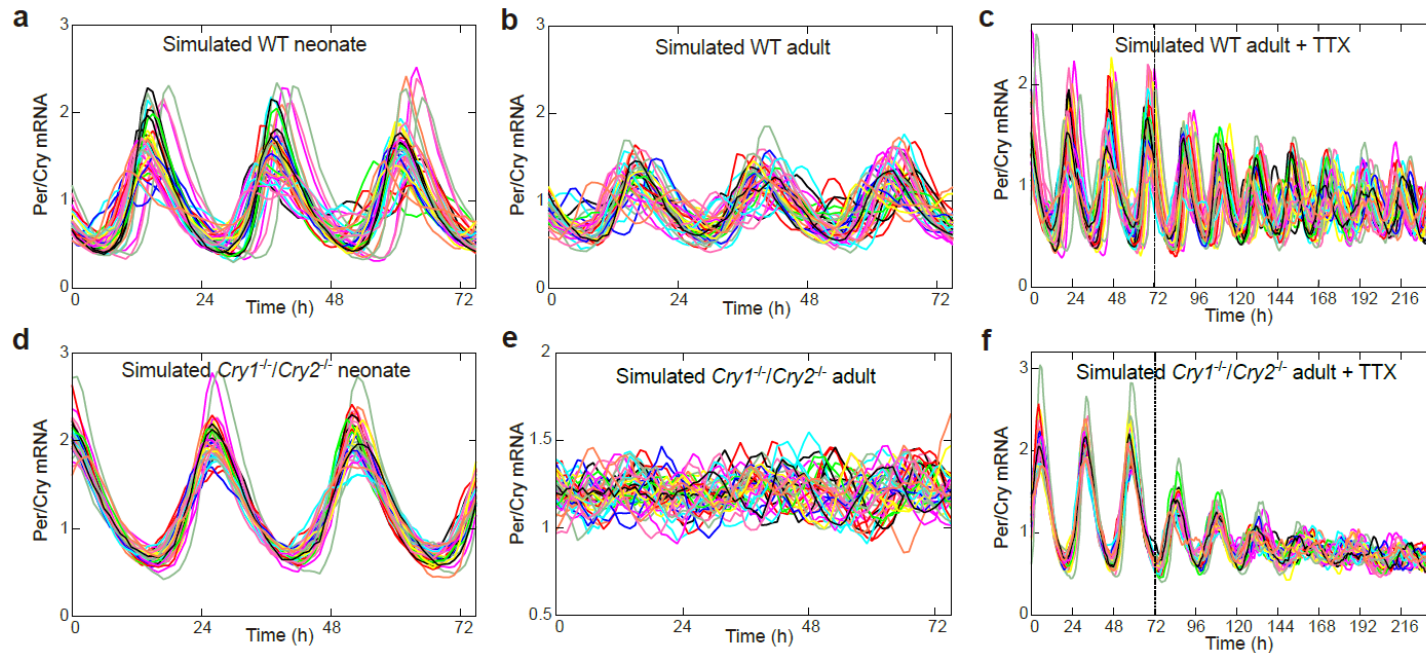


Implications for dual role of GABA (J. Evans, Neuron 2013) and synchrony of neonatal versus adult SCN slices (Honma, Nature Communications 2013)

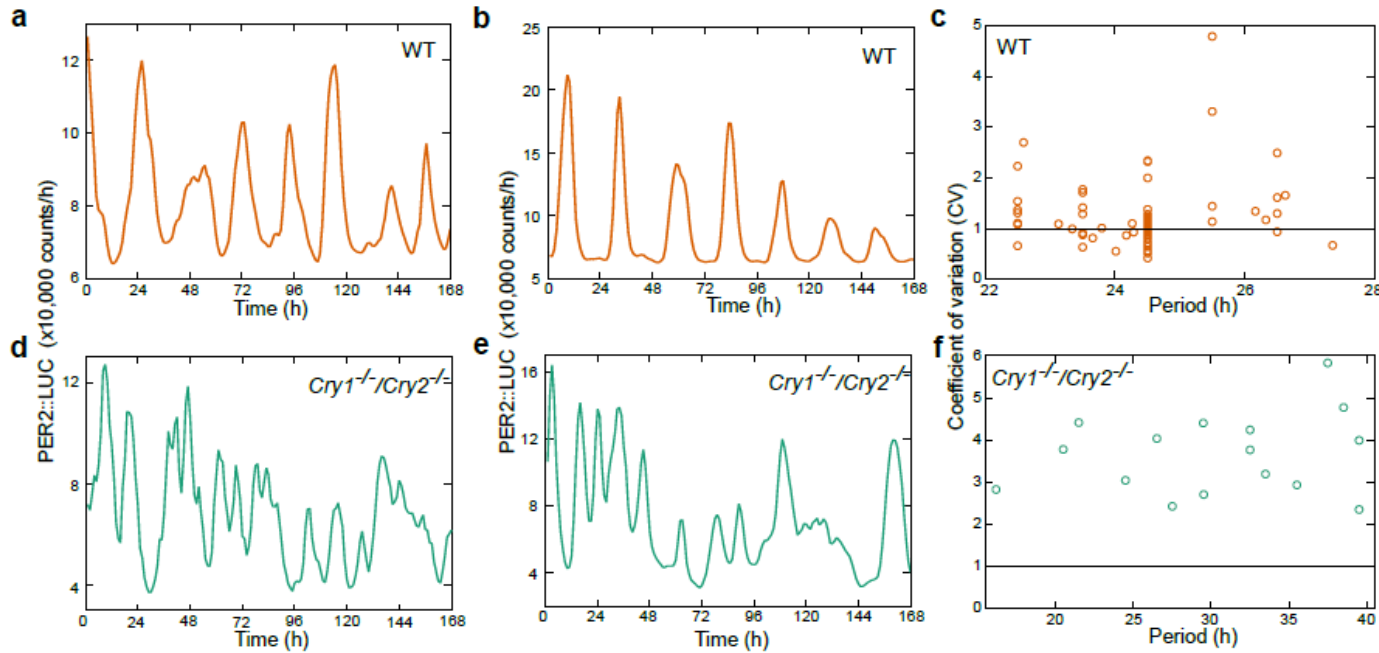
SCN slice data from wildtype and knockouts



Network simulations with varying coupling phases

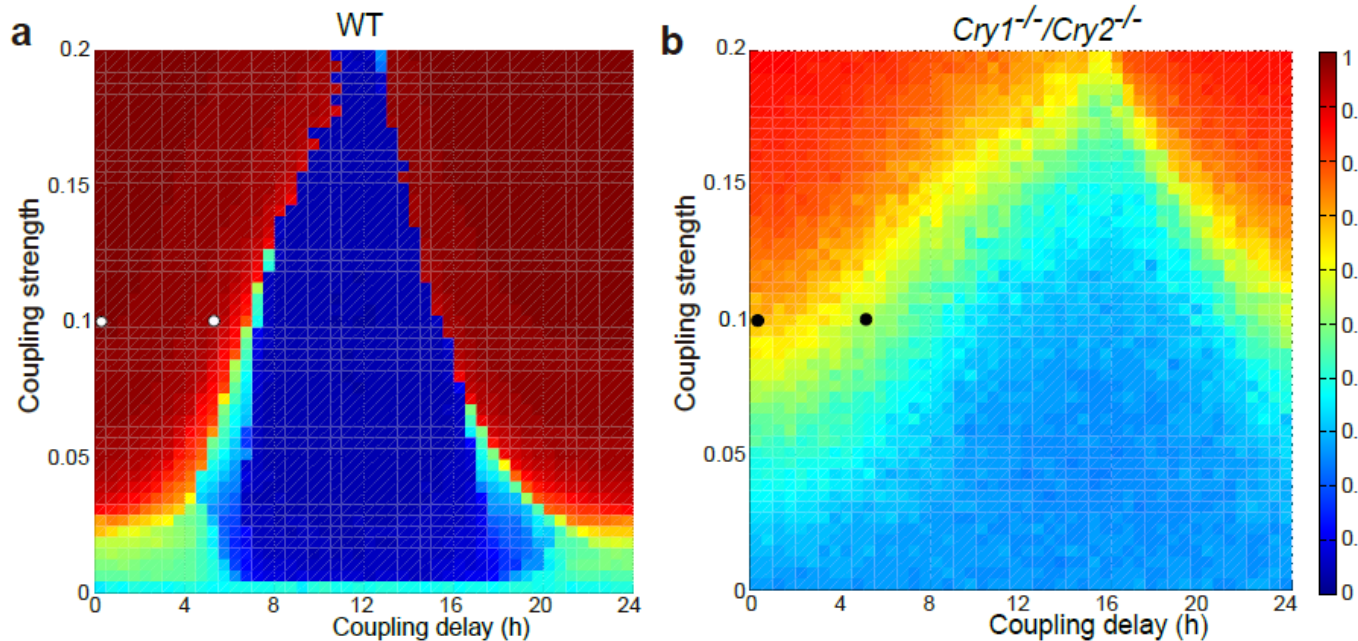


Synchronization of noisy oscillators (WT and DKO)



CV about 1

CV above 1



Better sync for WT

Coupling strength enhances sync

Coupling phase matters strongly

Part 2: Summary and outlook

- Many SCN neurons might be noisy weakly damped oscillators
- Ensembles of damped oscillators are easily synchronized and entrained
- Coupling phase as essential as coupling strength

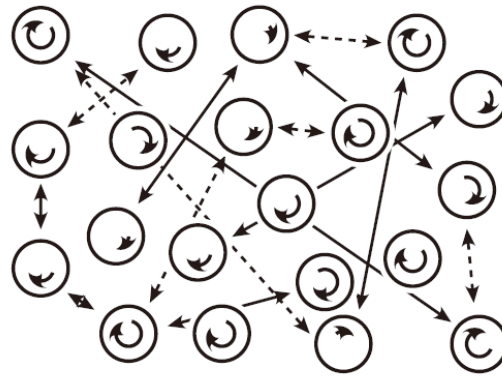
Outlook:

- Dominant coupling mechanisms?
- Quantification of coupling strength?
- Role of spatial heterogeneities?
- Control of entrainment phases („chronotypes“)

Outline

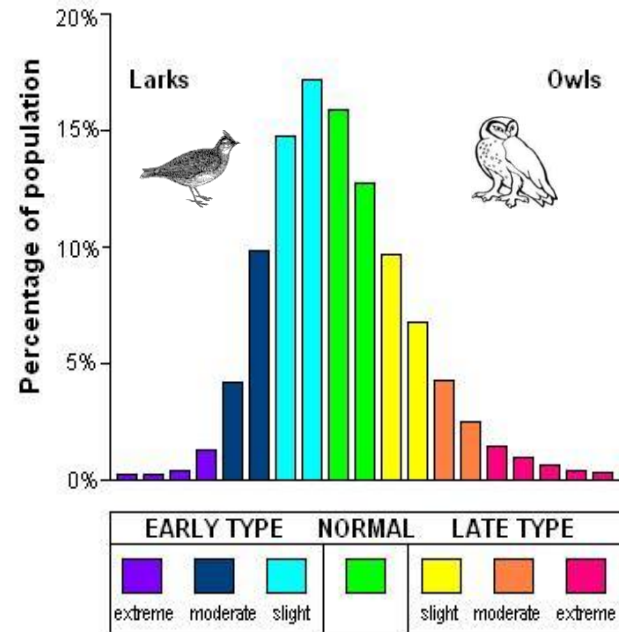
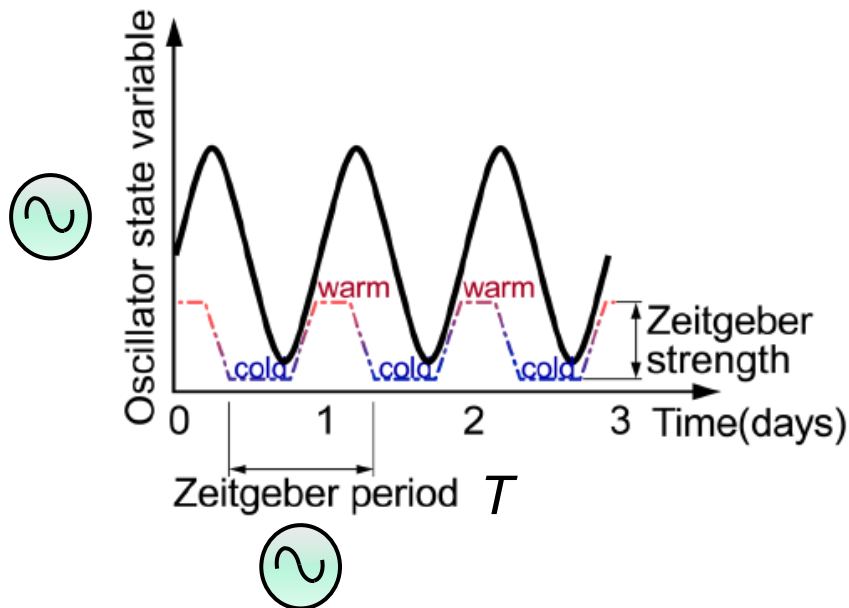
1. Synergy of feedback loops

2. Oscillator networks



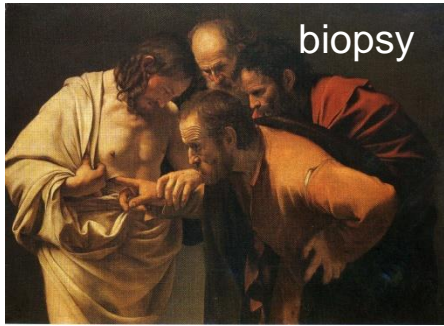
3. Entrainment phase (chronotypes)

Hallmarks of entrainment

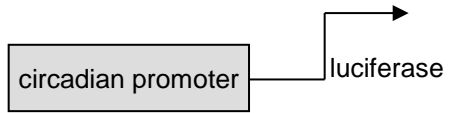


Period of the entrained oscillator becomes equal to the Zeitgeber period

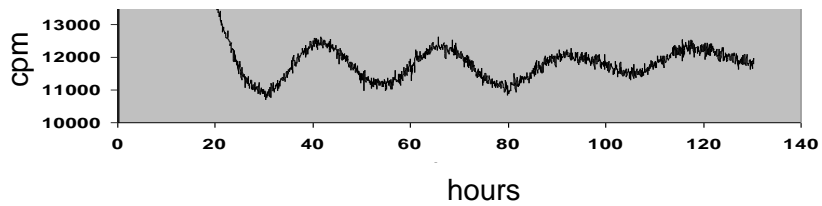
The phase-angle between Zeitgeber cycle and entrained oscillator is constant (i.e. **the phase of entrainment \leftrightarrow chronotype**)



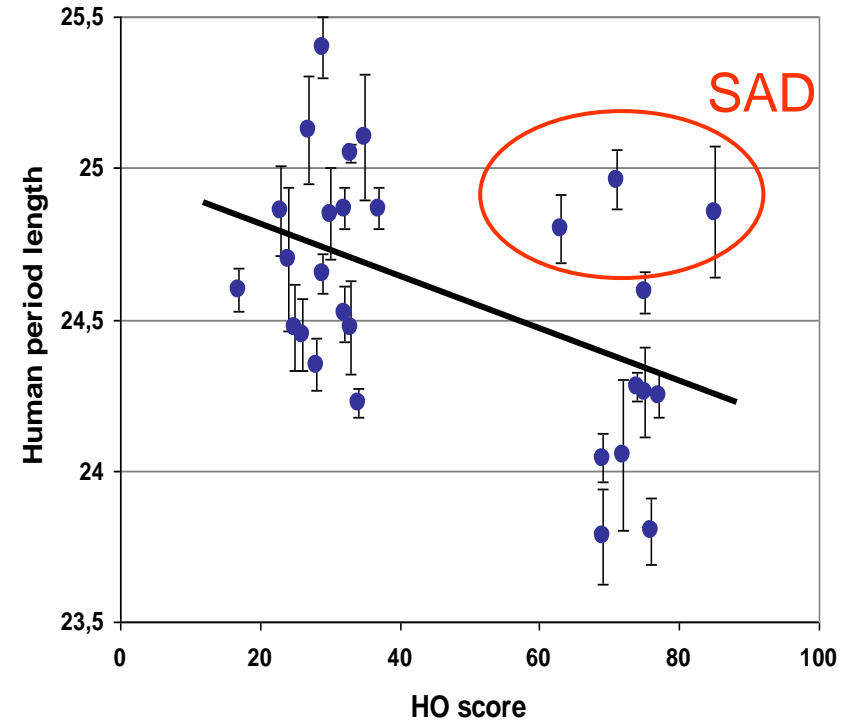
skin fibroblasts



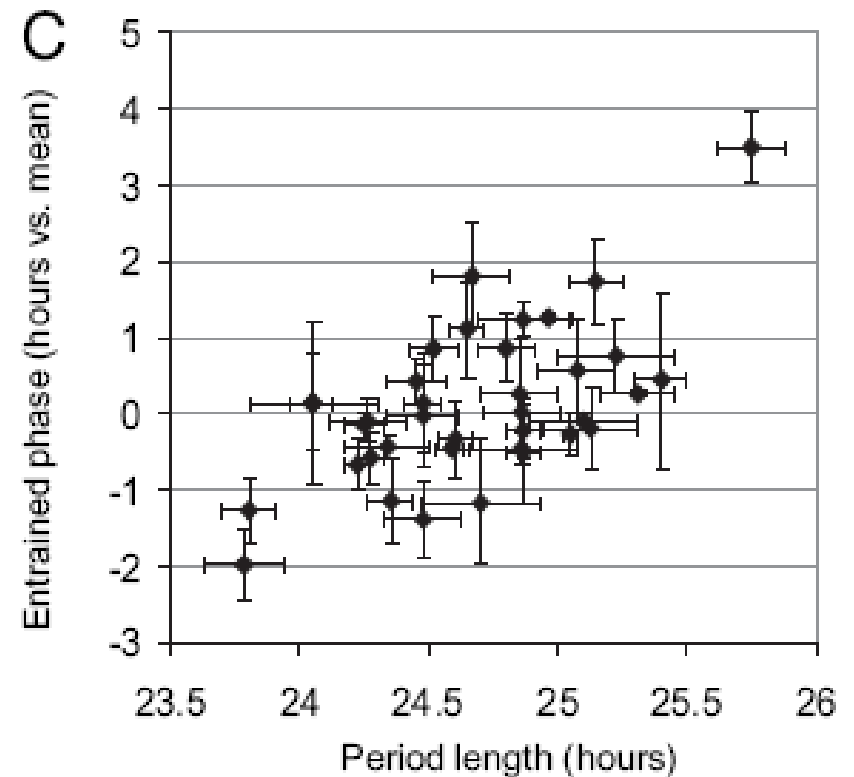
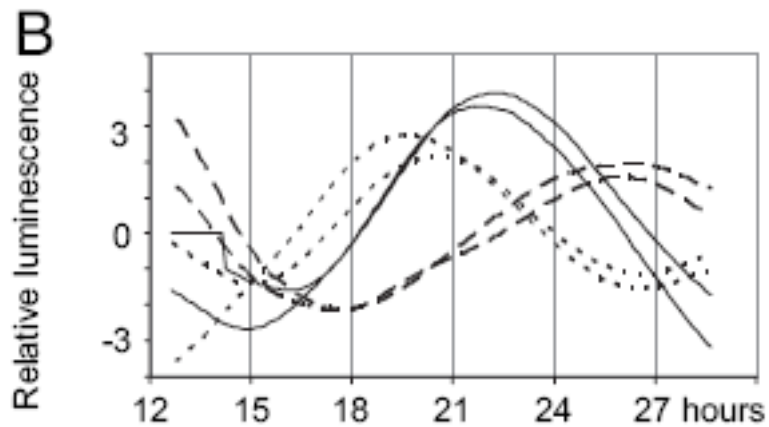
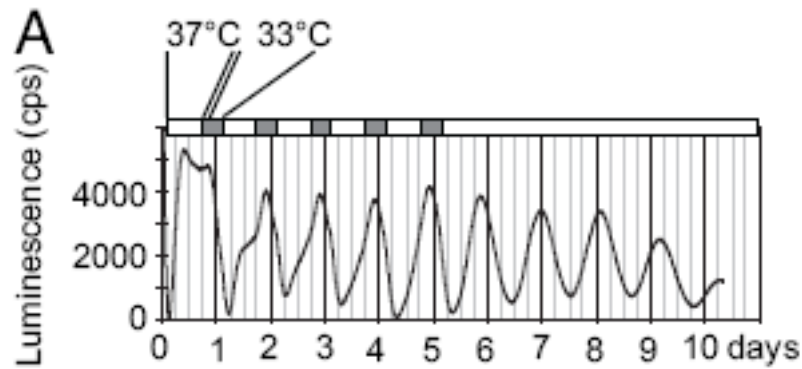
lentiviral infection



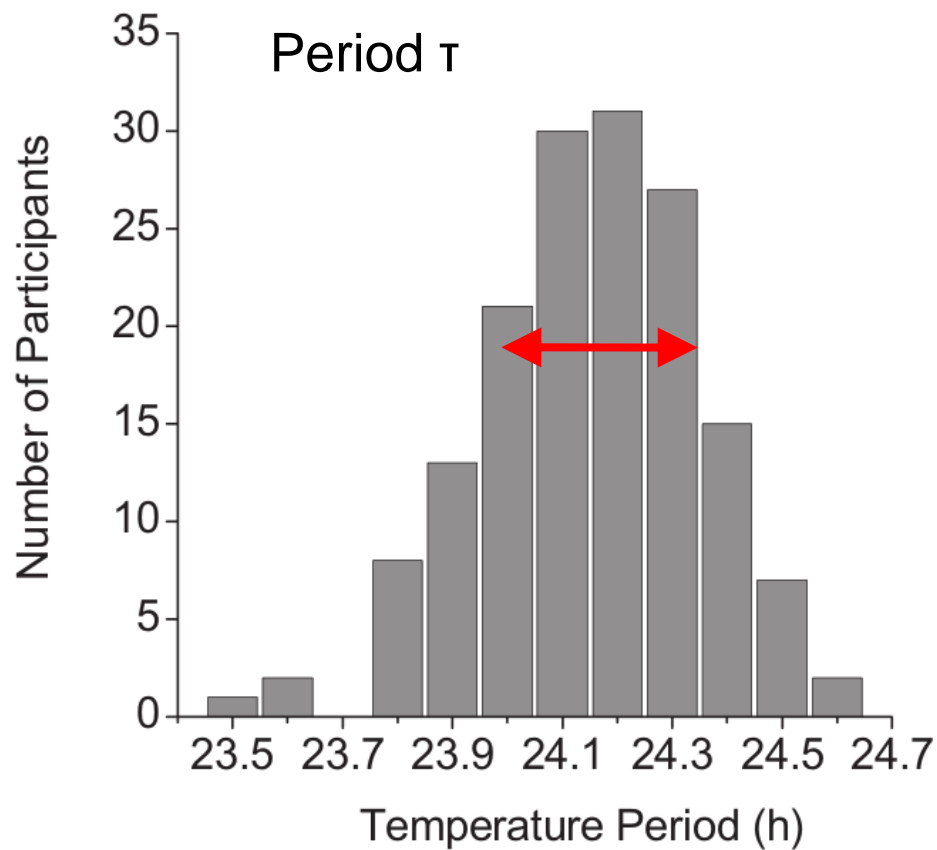
Direct measurement of human circadian period!



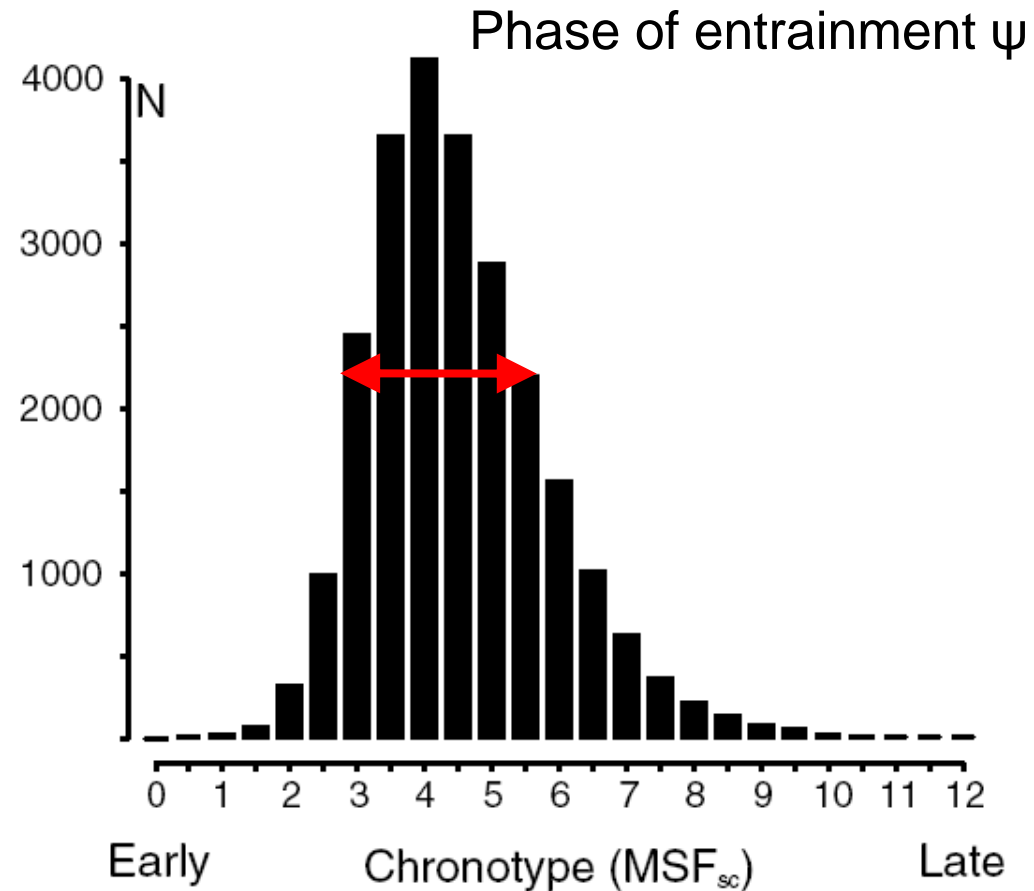
Fibroblast Period Length and Fibroblast Transcriptional Phase Correlate Under Entrained Conditions



Circadian period τ , phase of entrainment ψ in humans



Duffy et al., and Czeisler, 2011

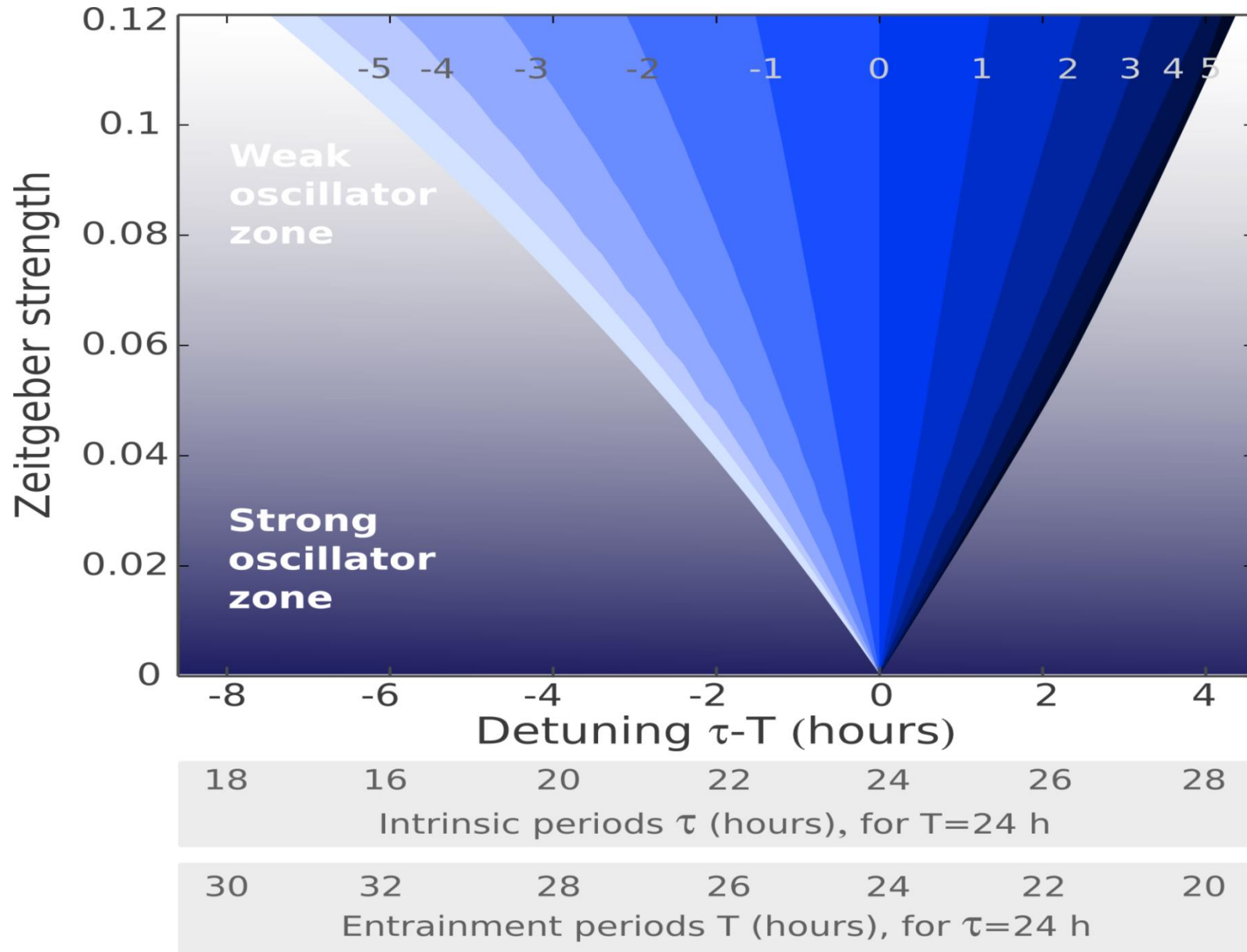


Roenneberg (2004)

small variations in τ (± 0.2 hrs) and wide range of chronotypes (± 1.5 hrs)

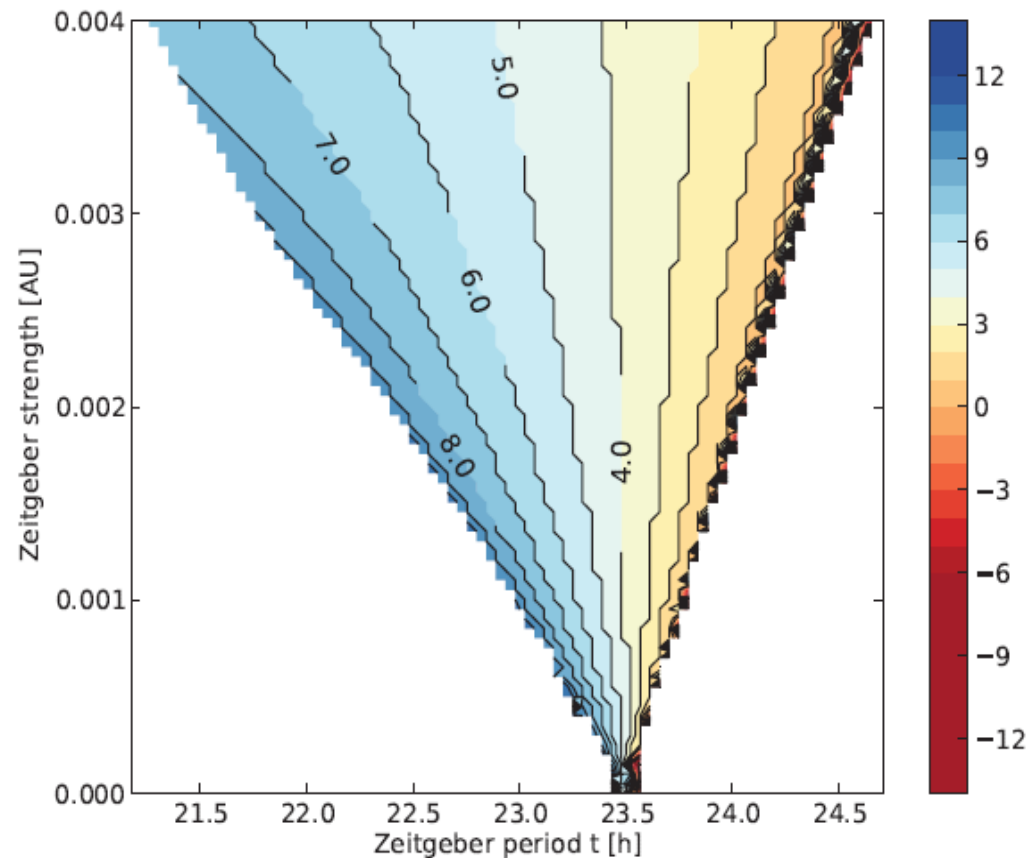
\rightarrow 7-fold ratio of $\Delta\psi$ to $\Delta\tau$

Small entrainment range implies large phase variability

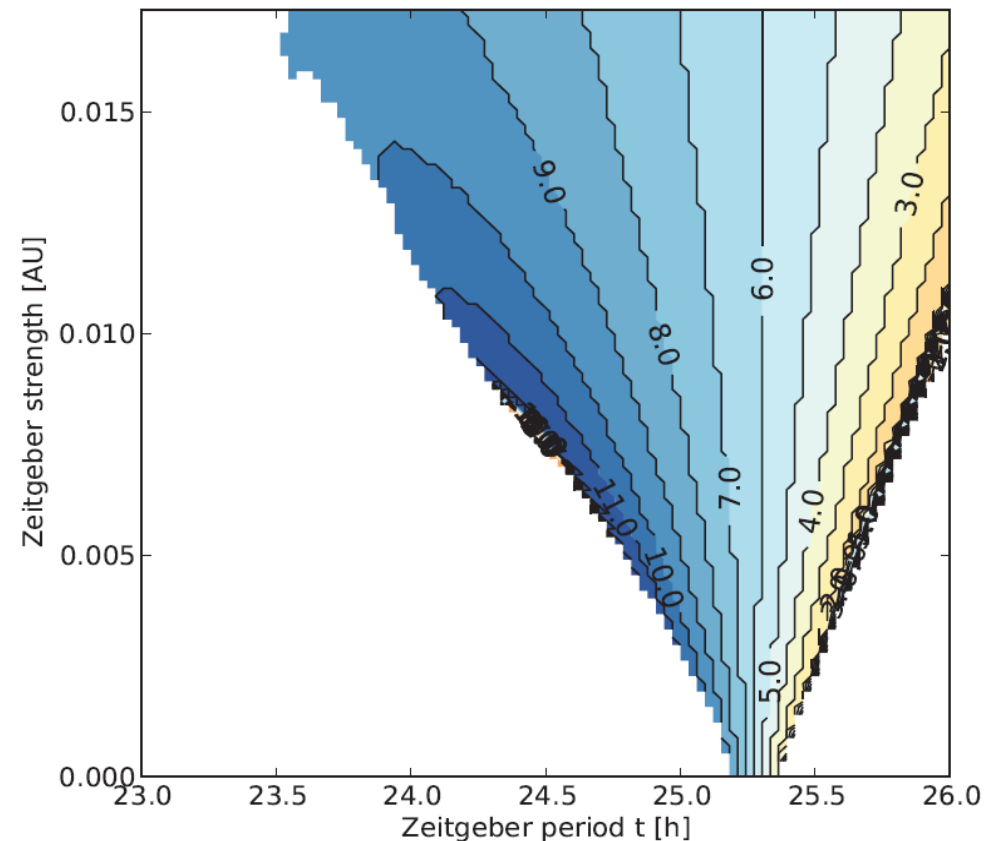


Test of theory using genetic network models

Katharina Imkeller, Master thesis 2013



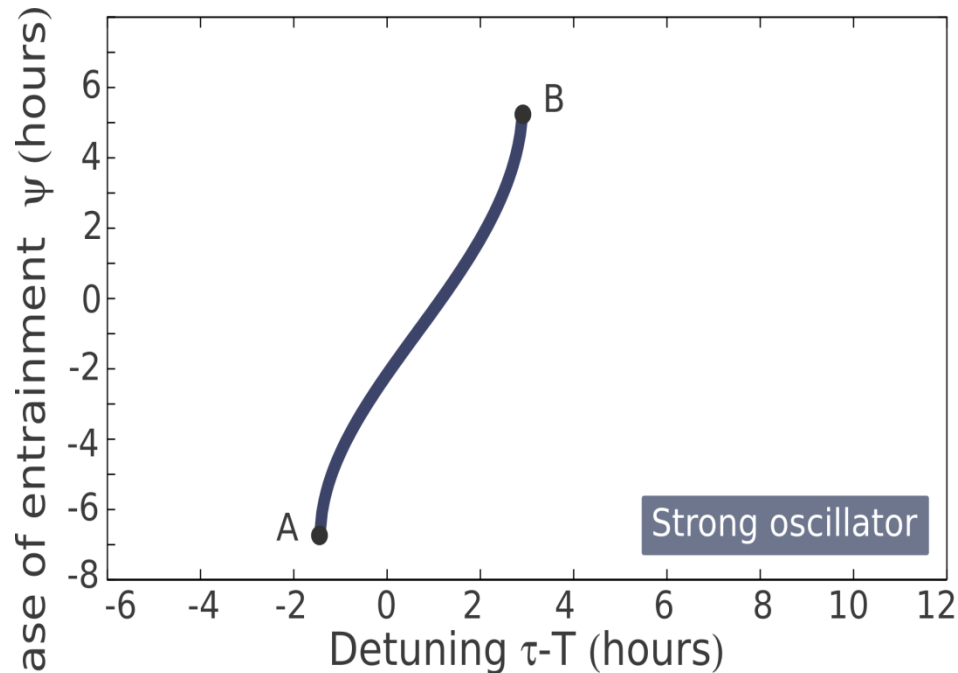
modified Goodwin model (3 ODEs)
Gonze et al. Biophys. J. 89 (2005)



two-loop model (19 ODEs) Religio
et al. PLoS Comp. Biol. 7 (2011)

Entrainment phase as a function of mismatch

large phase variations



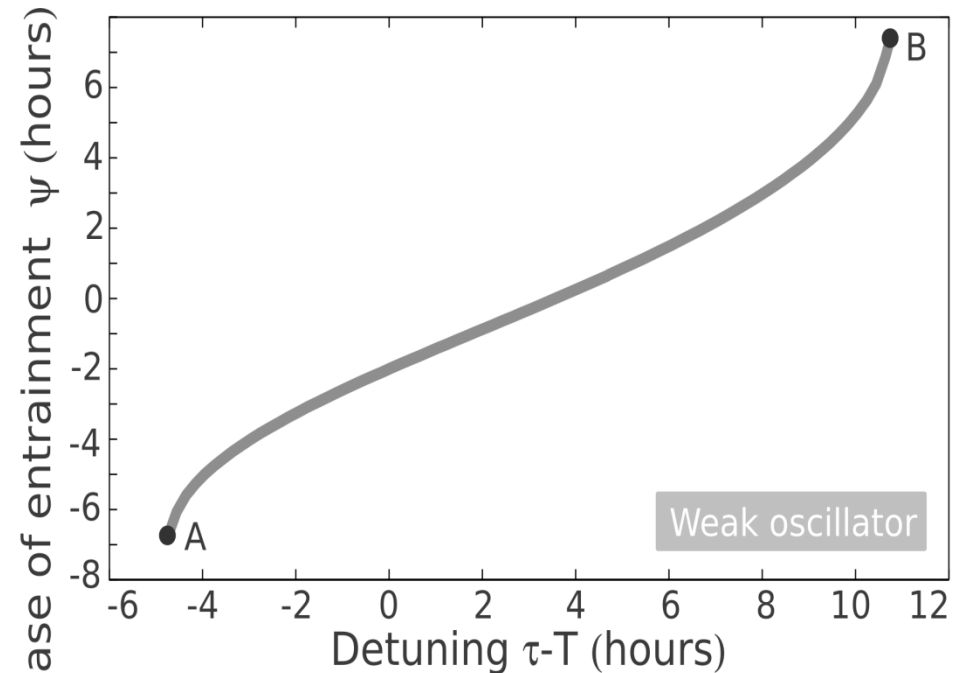
18 20 22 24 26 28 30 32 34 36

Intrinsic periods τ (hours), for $T=24$ h

30 28 26 24 22 20 18 16 14 12

Entrainment periods T (hours), for $\tau=24$ h

smaller phase variability



18 20 22 24 26 28 30 32 34 36

Intrinsic periods τ (hours), for $T=24$ h

30 28 26 24 22 20 18 16 14 12

Entrainment periods T (hours), for $\tau=24$ h

Increasing entrainment range and phase variability with Zeitgeber strength in lizards

102

K. HOFFMANN:

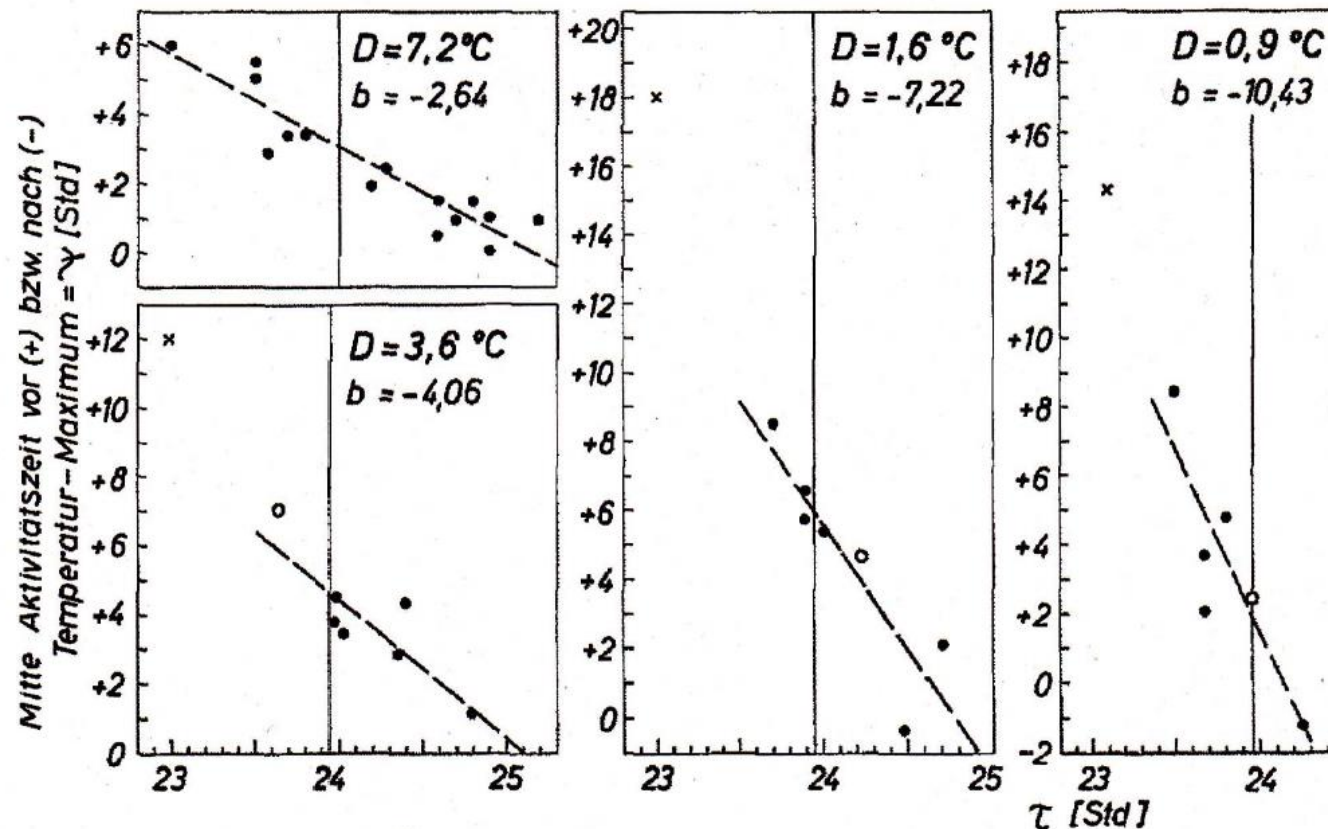


Abb. 5. Phasenwinkeldifferenzen zwischen Temperaturcyclus und biologischer Periodik in Abhängigkeit von der Spontanperiode der circadianen Periodik für vier Temperaturcyclen. Die berechneten Regressionsgeraden sind gestrichelt eingezeichnet ($b = b_{x,y}$). Man erkennt, daß sie mit abnehmender Amplitude des Temperaturcyclus steiler werden. Die — zur Berechnung der Regressionsgeraden nicht heran-

PRC/PTC as iterated map: stable entrainment phase varies by 12 hours

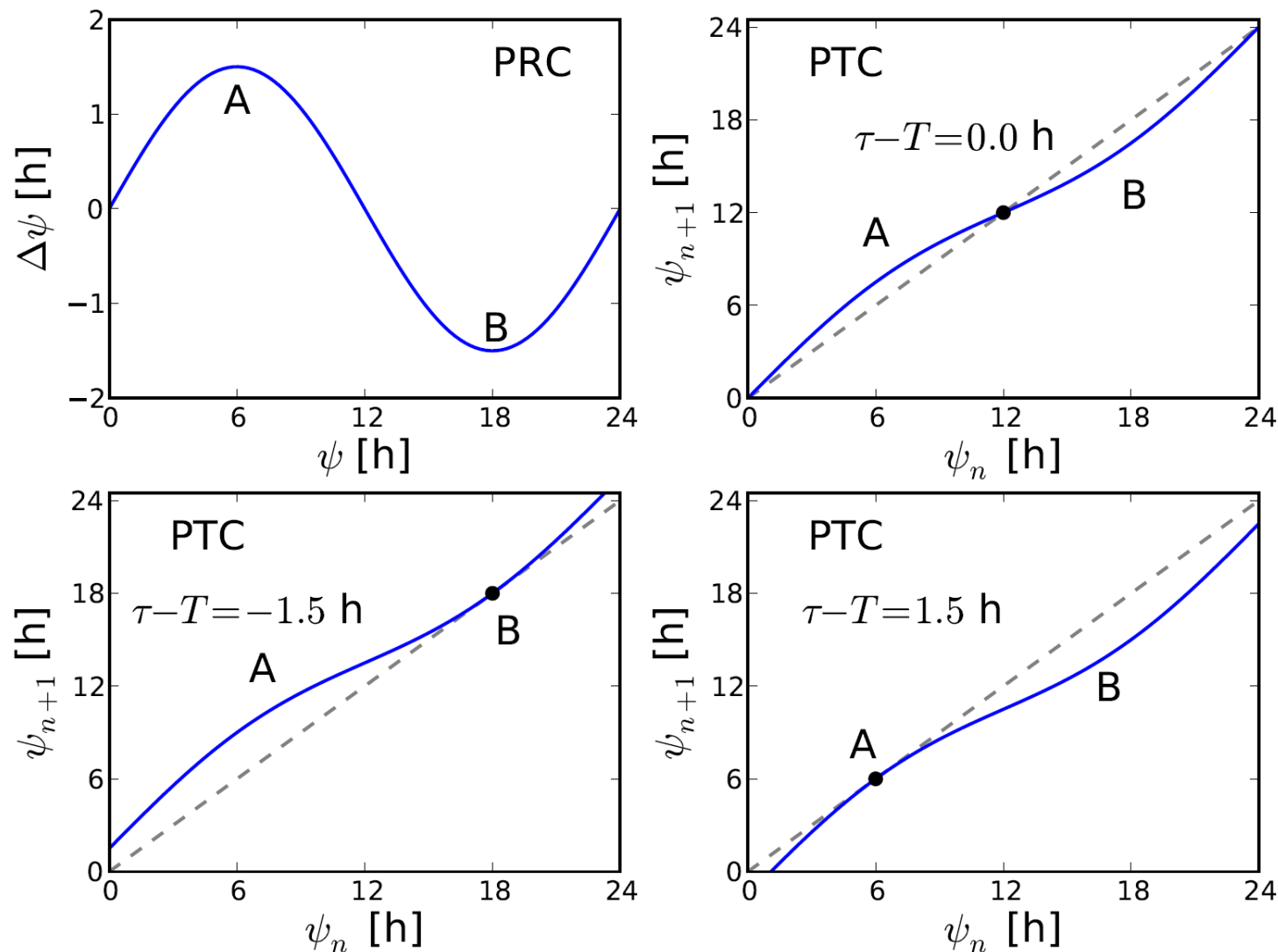


Figure 5: Sinusoidal phase response curve (PRC) and associated phase transition curves (PTCs) according to Eq. (5). Applying T -periodic pulses, stationary entrainment phases are given by the intersections of the PTC with the diagonal $\psi_{n+1} = \psi_n$ (Glass and Mackey, 1988). Upper graphs: Vanishing frequency mismatch $\Omega = 0$ leads to a stable entrainment phase $\psi = 12$ h. Lower graphs: Period mismatches $\tau - T = \pm 1.5$ correspond to the borderlines of the entrainment range. The corresponding entrainment phases of 18 h and 6 h are associated to the extrema of the sin-function and are 12 h (or 180°) apart.

Periodically driven damped oscillators exhibit phase jump of 180° around resonance

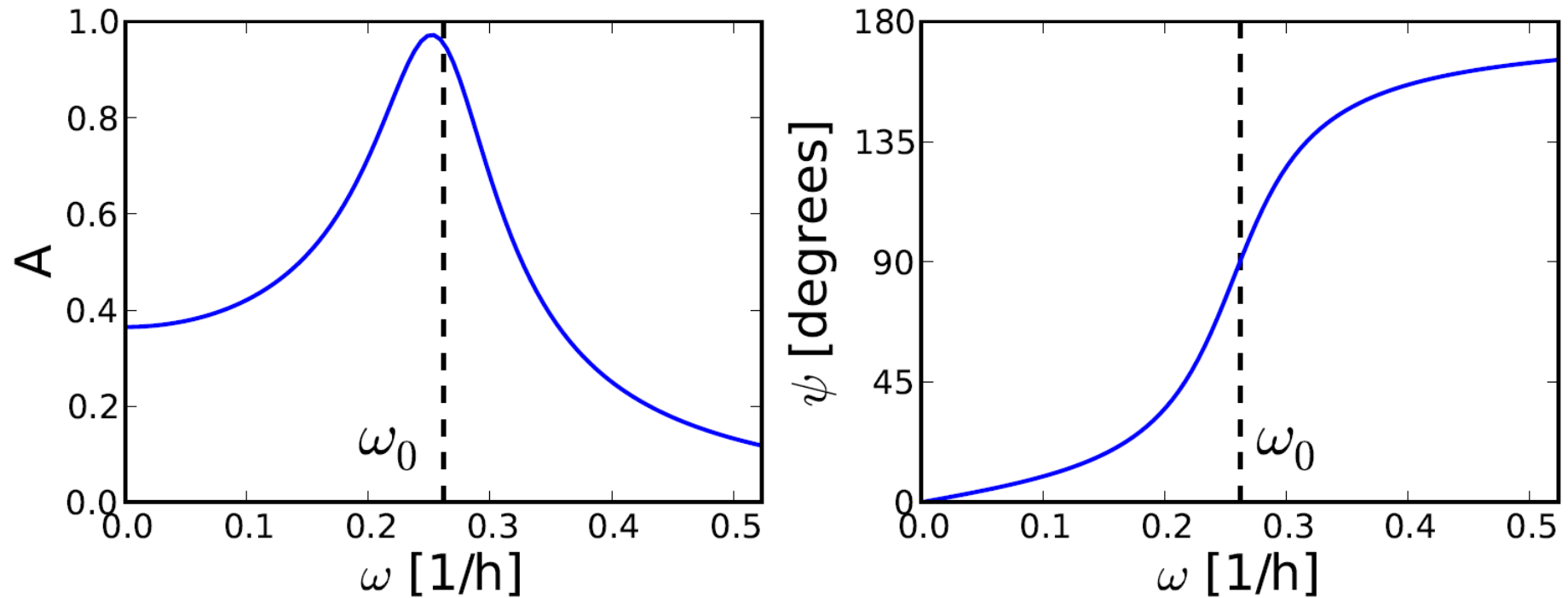
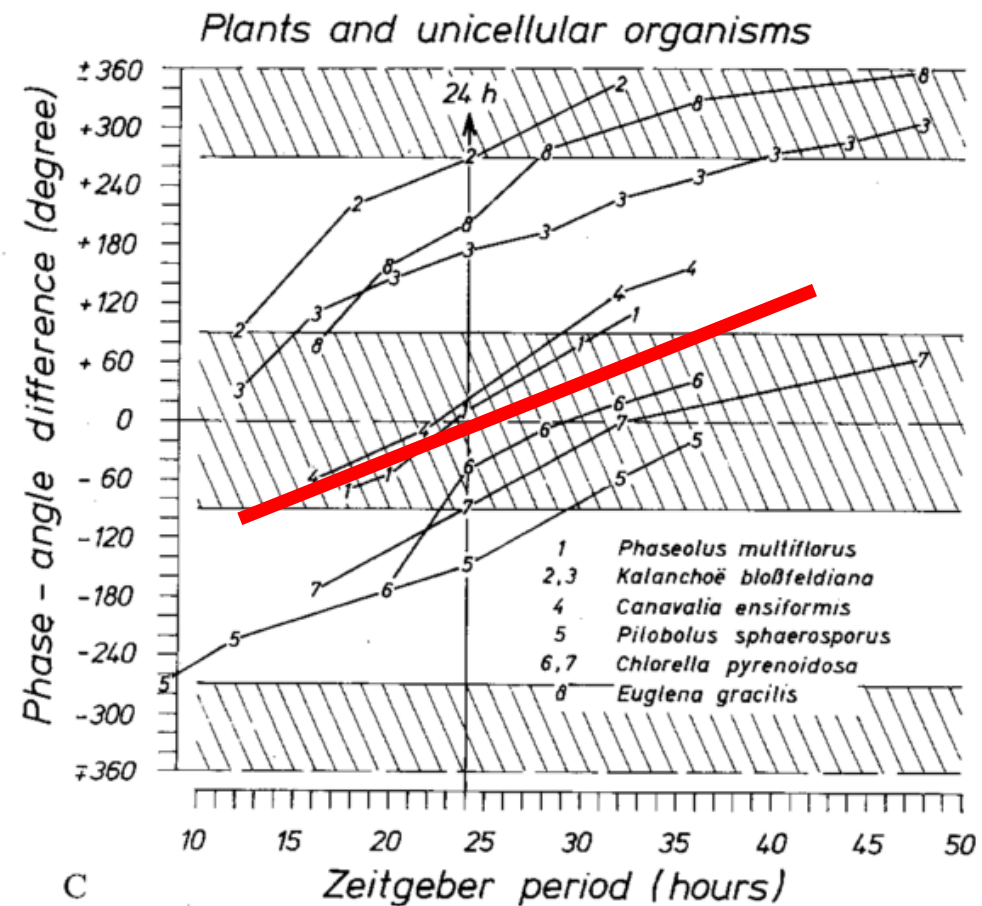
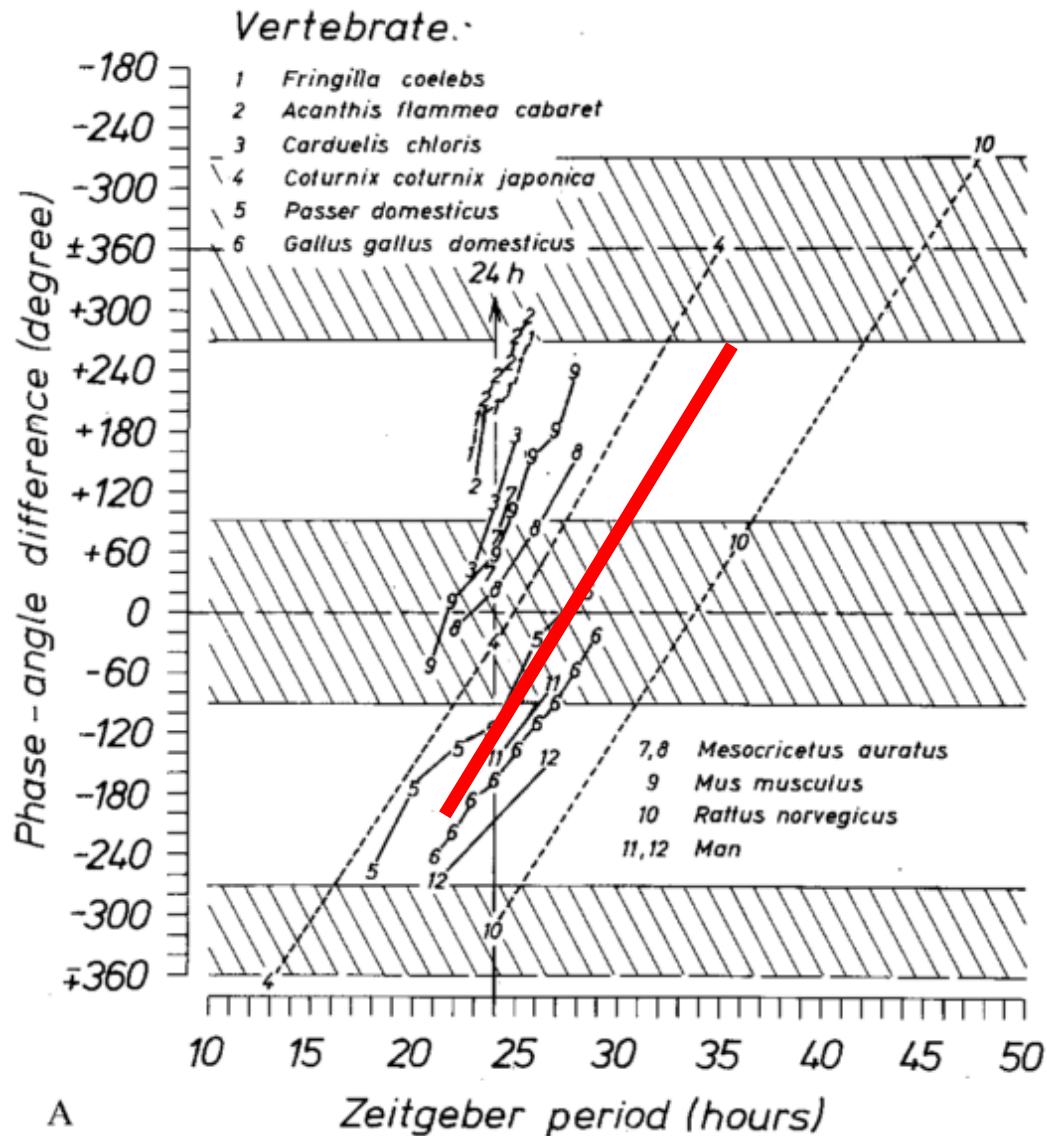
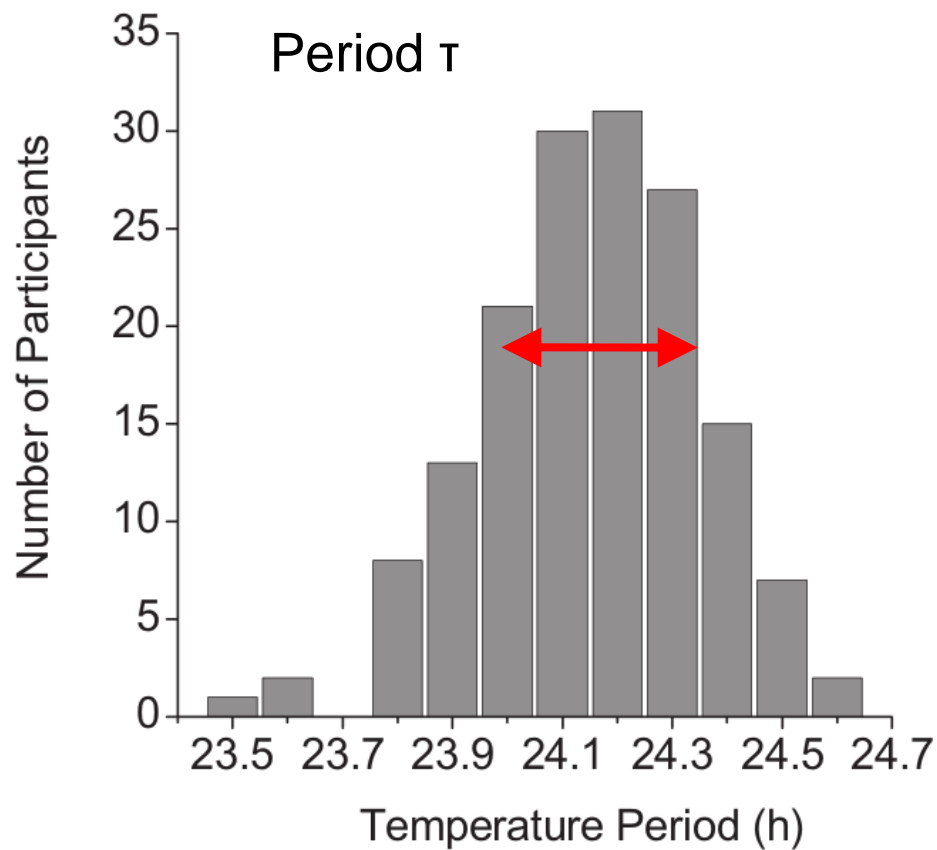


Figure 6: Amplitude and phase of a periodically driven weakly damped oscillator. The amplitude (left) shows a resonance peak near the intrinsic frequency $\omega_0 = \frac{2\pi}{24}$. Near the resonance the phase difference between the oscillator and the driver is changing by about 180° (right).

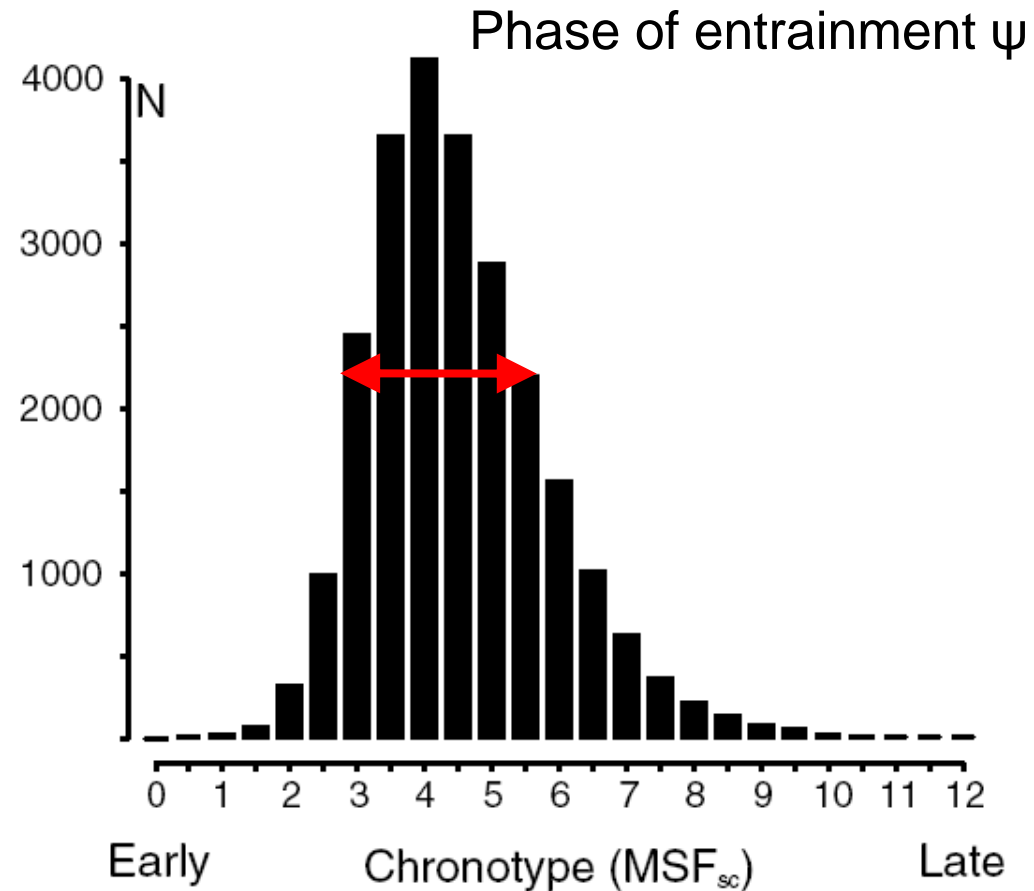
Uncoupled circadian systems have a smaller ratio of $\Delta\psi$ to $\Delta\tau$



Circadian period τ , phase of entrainment ψ in humans



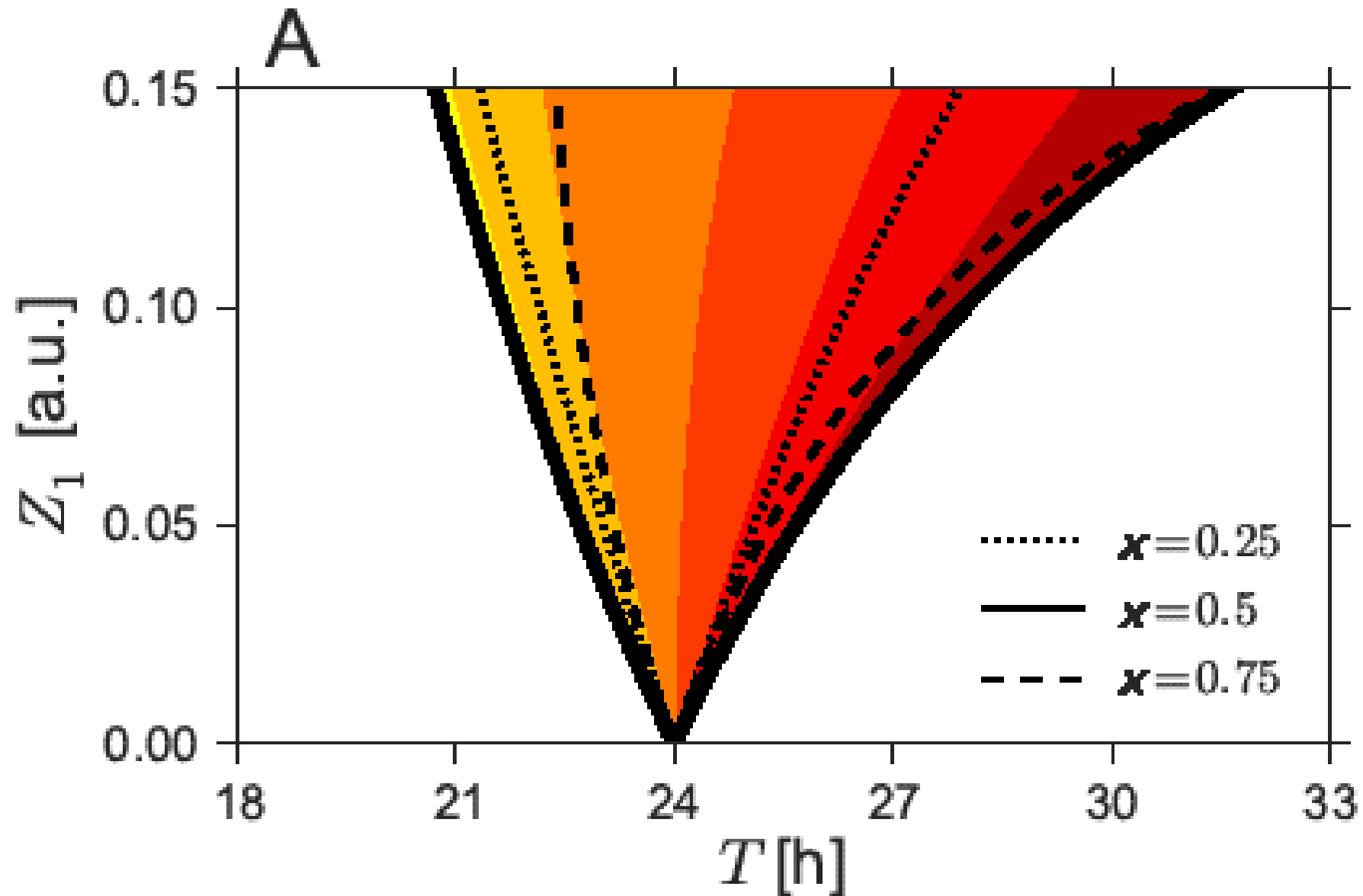
Duffy et al., and Czeisler, 2011



Roenneberg (2004)

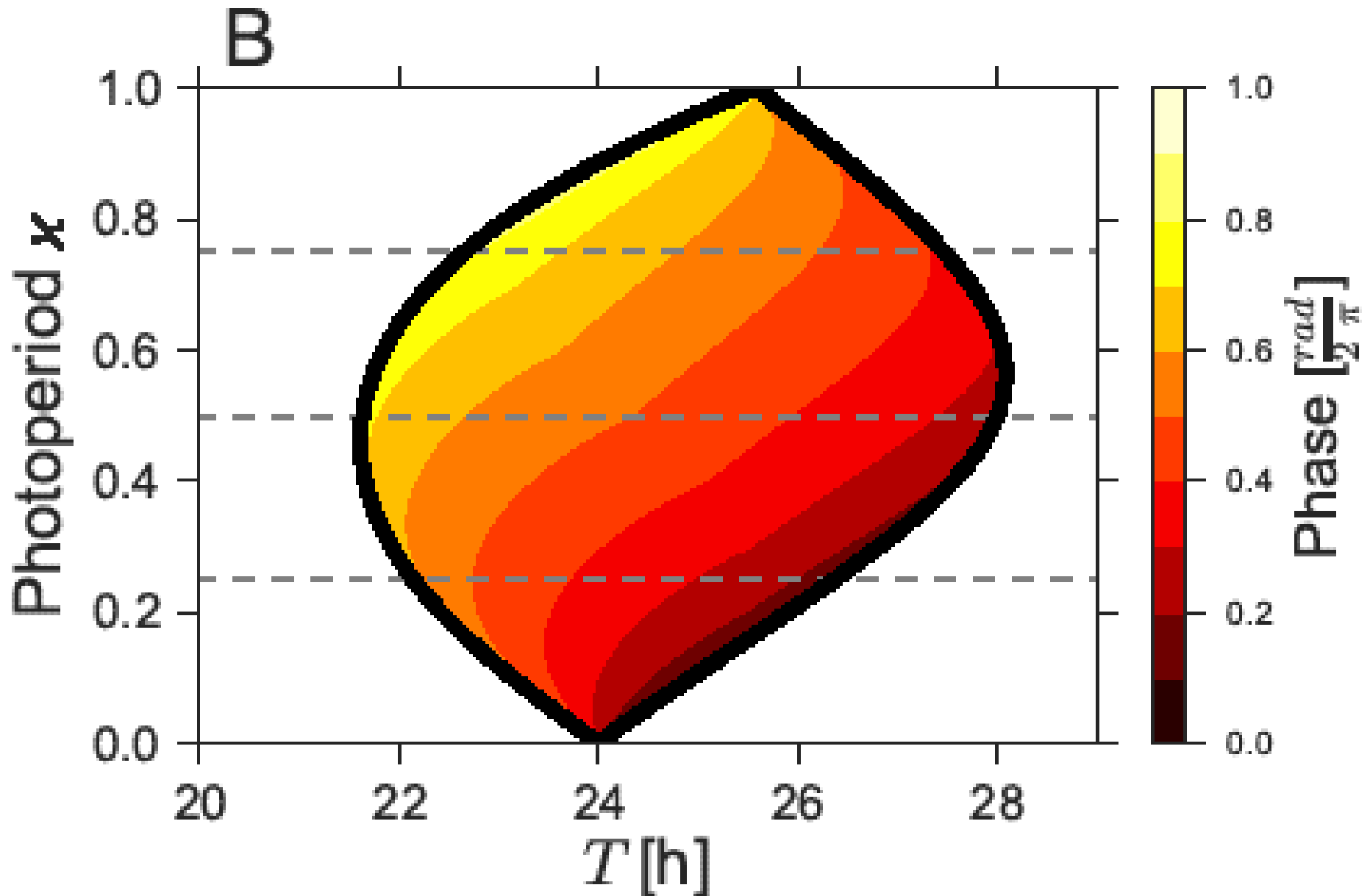
small variations in τ (± 0.2 hrs) lead to wide range of chronotypes (± 1.5 hrs)
since the SCN is a „strong oscillator“ due to coupling

Photoperiod (day length) effects entrainment range



Simulations of amplitude-phase oscillator (C. Schmal et al. 2015)

Arnold onion quantifies seasonality



Summary Part 3

- Coupling leads to „strong oscillators“ with small PRC, narrow entrainment range and variable phases
- Models predict dependencies of entrainment phases on period mismatch, Zeitgeber strength/amplitude and photoperiods
- Theory explains wide range of chronotypes (see also Wever 1964)
- Mammals: Robust oscillator implies flexible phase